University of Alberta

Characterization of the Interaction Between Intact Hemoglobin and the Anticancer Drug Oxaliplatin Using Nanoelectrospray Ionization Mass Spectrometry

by

Jun Peng

A thesis submitted to the Faculty of Graduate Studies and Research in partial fulfillment of the requirements for the degree of *Master of Science*

in

Medical Sciences-Public Health Sciences

Edmonton, Alberta

Fall 2005

Library and Archives Canada

Published Heritage Branch

395 Wellington Street
Ottawa ON K1A 0N4
Canada

Bibliothèque et Archives Canada

Direction du Patrimoine de l'édition

395, rue Wellington
Ottawa ON K1A 0N4
Canada

Your file Votre référence
ISBN: 0-494-09263-7
Our file Notre référence
ISBN: 0-494-09263-7

NOTICE:
The author has granted a non-exclusive license allowing Library and Archives Canada to reproduce, publish, archive, preserve, conserve, communicate to the public by telecommunication or on the Internet, loan, distribute and sell theses worldwide, for commercial or non-commercial purposes, in microform, paper, electronic and/or any other formats.

The author retains copyright ownership and moral rights in this thesis. Neither the thesis nor substantial extracts from it may be printed or otherwise reproduced without the author's permission.

AVIS:
L'auteur a accordé une licence non exclusive permettant à la Bibliothèque et Archives Canada de reproduire, publier, archiver, sauvegarder, conserver, transmettre au public par télécommunication ou par l'Internet, prêter, distribuer et vendre des thèses partout dans le monde, à des fins commerciales ou autres, sur support microforme, papier, électronique et/ou autres formats.

L'auteur conserve la propriété du droit d'auteur et des droits moraux qui protège cette thèse. Ni la thèse ni des extraits substantiels de celle-ci ne doivent être imprimés ou autrement reproduits sans son autorisation.

In compliance with the Canadian Privacy Act some supporting forms may have been removed from this thesis.

While these forms may be included in the document page count, their removal does not represent any loss of content from the thesis.

Conformément à la loi canadienne sur la protection de la vie privée, quelques formulaires secondaires ont été enlevés de cette thèse.

Bien que ces formulaires aient inclus dans la pagination, il n'y aura aucun contenu manquant.

Canada

Abstract

The quaternary structure of hemoglobin (Hb) is important to its functions in biological systems. Therefore, it is advantageous to study the intact Hb tetramer instead of its subunits in order to study the modification of Hb due to chemical interactions in biological systems, for example, drug interactions. A nanoelectrospray ionization tandem mass spectrometry method was developed to simultaneously detect the noncovalently bound species: Hb tetramer and the glycated Hb. This method was further applied to study the interaction between the anticancer drug oxaliplatin and the Hb in a model incubation system and in blood of cancer patients undergoing oxaliplatin treatment. The intact Hb-oxaliplatin complexes were detected in the red blood cells of cancer patients and the structure was characterized using tandem MS: both parent drug and its hydrated species bind to the Hb. This study demonstrates the utility of mass spectrometry characterization of interactions of intact Hb tetramer with drugs in clinical studies.

Acknowledgements

First, I would very much like to thank Professor Xing-fang Li for her supervision, guidance, and support throughout my graduate studies. I really appreciate her leading me in the right direction in pursuit of good science. I would also like to thank Professor X. Chris Le for giving me a chance to study in this program and his invaluable advice as my supervision committee member. I would also like to thank Dr. Rupasri Mandal for her help throughout my projects. Thank you to the rest of the Environmental Health Lab personnel and staff for all of your assistance. I would also like to thank Professor Liang Li and Professor Jonathan Martin for their willingness to be my thesis examination member and their helpful advice.

I would like to gratefully acknowledge the contribution of Dr. Rupasri Mandal to tandem MS studies of intact Hb tetramer-drug complexes (Mass spectra were acquired in Sciex). I also thank Dr. Michael Sawyer and Beverly Larson of Cross Cancer Institute (Edmonton, Alberta, Canada) for their assistance with blood collection and blood sample preparation. I also thank Dr. Jeff Guthrie, Dr. Hailin Wang and Ms. Katerina Carastathis for their suggestions and proofreading of my thesis.

I also want to express my thanks to the Natural Sciences and Engineering Research Council of Canada (NSERC) and by Alberta Health and Wellness for their financial support to my thesis research.

Finally, I would like to thank my wife Jing Qu for her continuing love and support, and my beautiful daughter Eileen for being the most amazing member of my family.

Table of Contents

CHAPTER 1 INTRODUCTION **1**

1.1 HEMOGLOBIN 1

1.1.1 Structure *1*

1.1.2 Function *4*

1.2 HEMOGLOBIN COMPLEX: A USEFUL BIOMARKER 4

1.2.1 Glycated Hb: Hb Complex of Glucose *4*

1.2.2 Hemoglobin Complexes of Environmental Toxicants *5*

1.3 INTERACTION OF HB WITH PLATINUM-CONTAINING ANTICANCER DRUGS 5

1.3.1 Platinum-Containing Drugs *6*

1.3.2 Oxaliplatin and Its Transformation Products *6*

1.3.3 Pharmacokinetics Study *8*

1.3.4 Toxicity *9*

1.3.5 Oxaliplatin-Protein Interactions *10*

1.4 CONVENTIONAL METHODS FOR ANALYSIS OF HB AND HB COMPLEXES 10

1.5 MASS SPECTROMETRY 11

1.5.1 Electrospray Ionization (ESI) *12*

1.5.2 Nanoelectrospray Ionization *15*

1.5.3 Quadrupole Mass Analyzer *16*

1.5.4 Time-of-Flight Mass Analyzer *17*

1.5.5 Hybrid Q-TOF Mass Spectrometer *18*

1.6 CHALLENGES IN ANALYSIS OF INTACT HB COMPLEXES BY MS 21

1.7 OBJECTIVES OF THE THESIS 21

REFERENCES 23

CHAPTER 2 DEVELOPMENT OF A NANOELECTROSPRAY IONIZATION MASS SPECTROMETRY METHOD FOR DETECTION OF INTACT HB TETRAMER AND GLYCATED HB 27

2.1 INTRODUCTION 27

2.2 EXPERIMENTAL 28

2.2.1 Materials and Sample Preparation 28

2.2.2 Instrumentation 29

2.3 RESULTS AND DISCUSSION 30

2.3.1 Effect of Sample Solution Composition 30

2.3.2 Sample Desalting 34

2.3.3 Effects of Instrumental Parameters on the Detection of the Hb Tetramer 37

2.3.3.1 Effect of Collision Energy 37

2.3.3.2 Effect of Declustering Potential and Focusing Potential 40

2.3.3.3 Effect of Collision Gas 44

2.3.4 Detection of the Intact Hb Tetramer and Glycated Hb 46

REFERENCES 49

CHAPTER 3 MASS SPECTROMETRIC STUDY OF INTERACTION BETWEEN INTACT HEMOGLOBIN AND OXALIPLATIN 51

3.1 INTRODUCTION 51

3.2 EXPERIMENTAL 52

3.2.1 Materials 52

3.2.2 Instrumentation *53*

3.2.3 Methods *54*

3.2.3.1 In vitro Incubation of Oxaliplatin with Hb 54

3.2.3.2 Red Blood Cell Lysis Methods 55

3.2.3.3 Patients' Blood Sample Preparation 55

3.3 RESULTS AND DISCUSSION 56

3.3.1 NanoESI-MS Study of Hb-Drug Complexes Formed in vitro *56*

3.3.2 Characterization of Hb-Oxaliplatin Complexes by Tandem MS *65*

3.3.2.1 Tandem MS Study of Hb Dimer-Oxaliplatin Complexes 65

3.3.2.2 Tandem MS Study of Hb Ttetramer-Oxaliplatin Complexes 71

3.3.3 Detection of Hb-Oxaliplatin Complexes in Patients' Blood Samples *76*

3.3.3.1 Comparison of Two Red Blood Cell Lysis Methods 76

3.3.3.2 Detection of Hb-Oxaliplatin Complexes in Patients' Blood Samples 78

COMPLEX FRAGMENTS **82**

3.3.4 Detection of Serum Albumin-Oxaliplatin Complexes in Patients' Plasma Samples *83*

REFERENCES 85

CHAPTER 4 SUMMARY AND FUTURE WORK **87**

List of Tables

Table 2.1	The measured and calculated m/z of the peaks in Figure 2.1b.
Table 2.2	Measured mass, calculated mass and mass accuracy for different Hb species detected at different DP1 and FP values.
Table 2.3	Calculated and measured molecular mass of HbA0 and glycated Hb
Table 3.1	Measured m/z value of Hb and the three new species in Figure 3.1
Table 3.2.	Measured mass-to-charge ratios and mass accuracy of the fragment ions of the drug complexes formed in the incubated solution of Hb and oxaliplatin (Figure 3.8).
Table 3.3	Measured mass-to-charge ratios and mass accuracy of the fragment ions of the intact Hb-oxaliplatin complexes formed in RBC (Figure 3.11).

List of Figures

Figure 1.1 Diagram of the quaternary structure of an intact Hb tetramer.

Figure 1.2 Two-dimensional drawing of heme coordinated to the histidine residue of the hemoglobin protein.

Figure 1.3 Chemical structure of oxaliplatin and its main transformation products.

Figure 1.4 Diagram of how ESI-MS analyzes a protein sample.

Figure 1.5 Schematic diagram of a quadrupole mass filter.

Figure 1.6 Diagram of the quadrupole/time-of-flight mass spectrometer (Applied Biosystems/MDS Sciex).

Figure 2.1 Typical nanoESI mass spectrum of 10 μM Hb in: a) 10% methanol solution containing 0.01% formic acid (pH 4), b) 5 mM aqueous ammonium acetate buffer (pH 6.5).

Figure 2.2 a) NanoESI mass spectrum of 10 μM Hb without desalting, b) nanoESI mass spectrum of 10 μM Hb after desalting, c) nanoESI mass spectrum of the filtrate (the fraction of molecular mass less than 10 KDa) using a Microcon YM-10 centrifugal filter.

Figure 2.3 NanoESI mass spectrum of 10 μM Hb in 5 mM ammonium acetate buffer using three different CE values: a) CE 11 eV, b) CE 4 eV, c) CE 3 eV. T = Hb tetramer; D = Hb dimer; M = Hb monomer

Figure 2.4 Deconvoluted mass spectrum of 10 μM Hb in 5 mM ammonium acetate using three different DP1 and FP values: a) DP1 65, FP 215; b) DP1 45, FP 180; c) DP1 30, FP 150. (αhβh)2 represents the intact heme-bound tetramer; (αhβh) represents the heme-bound dimer; α, β represent the α-globin chain and β-globin chain, respectively.

Figure 2.5 Mass spectra of 10 μM Hb in 5 mM ammonium acetate buffer using different CAD values: a) CAD 2, b) CAD 5, c) CAD 7. T = Hb tetramer; D = Hb dimer; M = Hb monomer

Figure 2.6 a) NanoESI mass spectrum of 10 μM HbA0 in 5 mM aqueous ammonium acetate buffer in the mass range 3300-3900 m/z; b) deconvoluted mass spectrum of HbA0 and glycated Hb.

Figure 3.1 Typical nanoESI mass spectra of oxaliplatin-Hb complexes formed in reaction mixtures of oxaliplatin and Hb at oxaliplatin:Hb molar ratio of a) 0:1 , b) 1:1 , c) 5:1 , d) 10:1 . The reaction mixtures of oxaliplatin and Hb were incubated at 37 °C for 24 hours. The additional peaks labelled 1, 2, and 3 indicate three different Hb-drug complex species.

Figure 3.2 Deconvoluted mass spectra of the Hb tetramer control and the reaction mixture of oxaliplatin with Hb at molar ratio 10:1 incubated for 24 hours. The mass difference between Hb-1drug complex and Hb is 307 Da, which corresponds to the calculated molecular mass of hydrated drug loss of 2 H_20: Pt(DACH)- (the calculated molecular mass 307.3 Da). The mass difference between Hb-2drug complex and Hb-1drug complex is 308, which also corresponds to the calculated molecular mass of hydrated drug loss of 2 H_20: Pt(DACH)-.

Figure 3.3 Typical nanoESI mass spectra of oxaliplatin-Hb complexes formed in reaction mixtures of oxaliplatin and Hb at oxaliplatin:Hb molar ratio of a) 0:1, b) 1:1, c) 5:1, and d) 10:1. The reaction mixtures were incubated at 37°C for 5 days. The peaks labelled 1, 2, 3, 4, 5, and 6 indicate the different species of Hb-1drug , Hb-2drug, Hb-3drug, Hb-4drug, Hb-5drug and Hb-6drug complex, respectively.

Figure 3.4 NanoESI mass spectrum of the Hb dimer and dimmer-oxaliplatin complexes formed in a reaction mixture of Hb with oxaliplatin molar ratio 1:1 incubated for 24 hours. The peaks at m/z 2480, 2504, 2686, and 2714 indicate the charge state 13+ and 12+ ions of the Hb dimer ($\alpha h \beta h$) and the Hb dimer-drug complexes, respectively.

Figure 3.5 Product ion spectra of a) precursor ions of Hb dimmer (m/z 2686) and b) precursor ion of dimmer-drug complex (m/z 2714) obtained at a collision energy of 80 eV and collision gas setting of 9.

Figure 3.6 Partial deconvoluted product ion spectrum of precursor ion m/z 2714 (from molecular mass 14500 to 18000 Da). The molecular mass of α-chain and α-drug is 15125.8 and 15433.0 Da, respectively, and the mass difference is 307.2 Da. The molecular mass of β-chain, β-drug is 15867.2 and 16174.6 Da, respectively, and the mass difference is 307.4 Da.

Figure 3.7 Product ion mass spectrum of precursor ion charge state 18+ of the Hb tetramer-oxaliplatin complexes a) at CE 15 eV; b) at CE 30 eV; c) expanded mass range to show the presence of parent drug oxaliplatin ions at CE 30 eV.

Figure 3.8 a) ESI mass spectrum of oxaliplatin control, b) product ion spectrum of charge 18+ Hb-drug complex, c) expanded product ion spectrum shows

additional fragment ions, which are [α-Pt(DACH)], [α-Pt(DACH)(Oxalate)] and [β-Pt(DACH)], [β-Pt(DACH)(Oxalate)].

Figure 3.9 NanoESI mass spectra of the hemolysate of RBCs from one healthy volunteer using two lysis methods: a) hypotonic solution method and b) freezing/thawing method.

Figure 3.10 NanoESI mass spectra of Hb-oxaliplatin complexes in RBCs hemolysate from a cancer patient's blood sample: a) normal control; b) collected 1 hour after infusion; c) collected 48 hours after infusion.

Figure 3.11 Product ion mass spectrum of the precursor ion charge state 18+ of the Hb tetramer-oxaliplatin complexes in a patient's blood sample.

Figure 3.12 NanoESI mass spectra of serum albumin-oxaliplatin complexes in plasma from the same cancer patient's blood sample collected 1 hour after infusion and 48 hours after infusion. Each arrow represents the each series of peaks of HSA-1drug complex.

List of Abbreviations

ESI	Electrospray Ionization
MS	Mass Spectrometry
ESI-MS	Electrospray Ionization Mass Spectrometry
NanoESI	Nanoelectrospray Ionization
Hb	Hemoglobin
HbA0	main adult human hemoglobin
HSA	Human Serum Albumin
Q-TOF	Quadrupole/time-of-flight
TOF	Time-of-flight
m/z	mass to charge ratio
Pt	platinum
T	Tetramer
D	Dimer
M	Monomer
FDA	Food and Drug Administration
ICP-MS	Inductively coupled plasma mass spectrometry
NMR	Nuclear Magnetic Resonance
Q0	Quadrupole0
Q1	Quadrupole1
Q2	Quadrupole2
DP	Declustering Potential
DP 1	Declustering Potential 1
FP	Focusing Potential
CE	Collision Energy
CAD	Collision Activated Dissociation
HPLC	High Performance Liquid Chromatography
RBC	Red Blood Cell
RBCs	Red Blood Cells
DACH	1,2-diaminocyclohexane

r.f.	radio frequency
ac	alternative current
dc	direct current
T19+	charge state 19+ ion of the Hb Tetramer
T18+	charge state 18+ ion of the Hb Tetramer
T17+	charge state 17+ ion of the Hb Tetramer
D13+	charge state 13+ ion of the Hb Dimer
D12+	charge state 12+ ion of the Hb Dimer
M9+	charge state 9+ ion of the Hb Monomer
M8+	charge state 8+ ion of the Hb Monomer

Chapter 1 Introduction

1.1 Hemoglobin

Hemoglobin (Hb) is the main intracellular protein of human red blood cells (RBCs), constituting approximately 33 percent of their contents [1]. It is one of the most extensively studied proteins and serves as a valuable model in understanding how a protein works in the body. Hemoglobin, as an important functional protein, continues to be of great interest to many researchers in biomedical research fields.

1.1.1 Structure

In the RBC of adult humans, the main form of hemoglobin is HbA0, which contains four subunits: two α- polypeptide chains and two β- polypeptide chains. Figure 1.1 shows the quaternary structure of the adult human HbA0.

The structure of a protein is described in terms of a hierarchy of structures: primary, secondary, tertiary, and quaternary. The primary structure is the sequence of amino acids along the polypeptide chain. The Hb α subunit (its identification number in the protein database Swiss-Prot is P01922) contains 141 amino acids and its molecular weight is 15126.4 Da. The β subunit (its identification number in Swiss-Prot is P02023) contains 146 amino acids and its molecular weight is 15867.2 Da [2]. The secondary structure refers to the local folding of the macromolecular backbone and can be specified by the angles between adjacent peptide groups. Proteins can form several different secondary structures, including the α-helix, β-sheet, and reverse turns [3]. The tertiary structure refers to the next order of folding of the polypeptide chain in which elements of

secondary structures are arranged with respect to one another. Proteins with more than one polypeptide chain have a quaternary structure, which refers to the number, type, and arrangement of the different polypeptide chains [3].

The quaternary structure of Hb is formed by two α polypeptide chains and two β polypeptide chains, which are held together by noncovalent interactions to form an intact tetramer. The noncovalent forces involved in protein structure include hydrophobic interactions, ionic bonds, hydrogen bonds, and Van der Waals attractions [4]. Hereafter, we refer to the quaternary structure of Hb as the intact Hb tetramer, a noncovalent protein complex.

Each subunit of Hb contains a prosthetic group, heme. The heme prosthetic group contains a reduced iron atom in a largely hydrophobic, planar porphyrin ring. An iron atom of the heme group is bound to the imidazole ring of a histidine residue of hemoglobin [5]. Figure 1.2 shows the two-dimensional drawing of heme coordinated to the histidine residue.

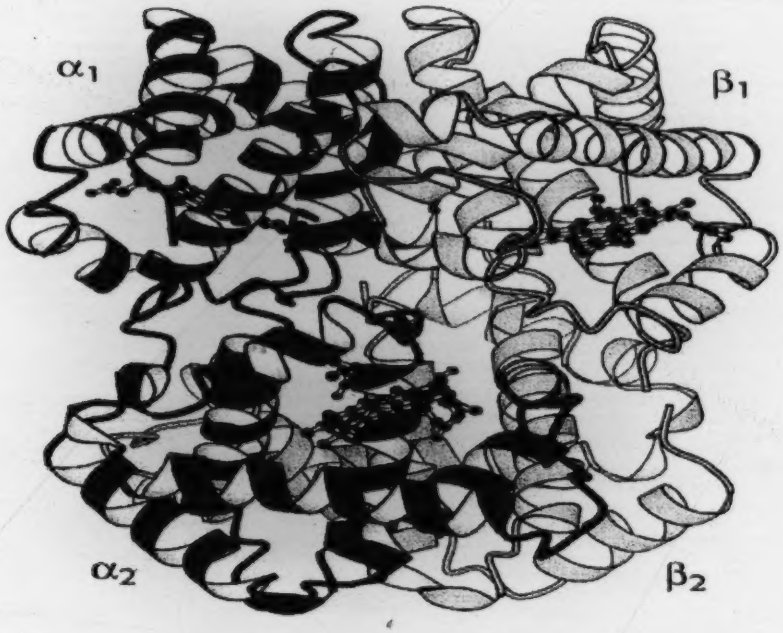

Figure 1.1 Diagram of the quaternary structure of an intact Hb tetramer.

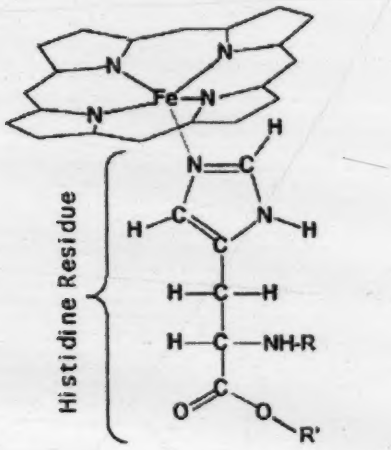

Figure 1.2 Two-dimensional drawing of heme coordinated to the histidine residue of the hemoglobin protein.

1.1.2 Function

Hb in the RBC carries oxygen from the lungs to the tissues and carries carbon dioxide from the tissues back to the lungs. Hb binds to oxygen tightly in the oxygen-rich atmosphere of the lungs and releases oxygen rapidly in the relatively oxygen-poor environment of the tissues [6]. The affinity of oxygen to hemoglobin is affected by pH, CO_2 and by the differences in the oxygen-rich environment of the lungs and the oxygen-poor environment of the tissues [6].

The quaternary structure of Hb is intimately related to its function. Each polypeptide chain contains one heme and each heme can bind to one oxygen molecule. Therefore, each Hb molecule can bind to four oxygen molecules. The affinity of any one subunit depends on the presence or absence of oxygen on the other subunits. Such variable affinity is known as cooperativity and is key to oxygen delivery by Hb [7].

1.2 Hemoglobin Complex: A Useful Biomarker

1.2.1 Glycated Hb: Hb Complex of Glucose

The major adult human hemoglobin is HbA0. During the life of the red blood cell, a small amount of modified forms of HbA0 could possibly exist. For instance, HbA1a, HbA1b, and HbA1c are produced by occasional chemical reactions with glucose and other compounds [8]. HbA1c is a glycosylated form of HbA0, which hereafter is called glycated Hb. The formation of HbA1c is directly related to the blood glucose concentration. The amount of HbA1c can be used to monitor the blood glucose amount in patients with diabetes mellitus. Because the normal regulation of the blood glucose concentration does not work in patients with diabetes mellitus, they must take care to

control their sugar intake directly. When the glucose concentration is high, the rate of formation of HbA1c is high and the level of HbA1c is increased. Because hemoglobin has a long lifetime (around 120 days), the proportion of Hb present as HbA1c may reflect the average glucose concentration over the lifetime of the red blood cell. Therefore, detection of glycated Hb is important because it can be used as a valuable biomarker of long-term diabetes control [9,10].

1.2.2 Hemoglobin Complexes of Environmental Toxicants

Protein complexes of environmental toxicants can be used as good biomarkers of exposure assessment and have applications in molecular epidemiological studies [11-13]. Because protein complexes are readily accessible, more abundant than DNA complexes, have a known rate of turnover and are not subject to enzymatic repair, protein complexes of environment toxicants are of great value as surrogates for DNA complexes and as suitable biomarkers of exposure assessment. For instance, hemoglobin, serum albumin, and histones were used as choice of proteins. Hemoglobin complexes of many environmental carcinogens, such as polycyclic aromatic hydrocarbons [14], 2-nitrotoluene [15], and butadiene [16], were identified and detected, and were applied as biomarkers in exposure monitoring and risk assessment.

1.3 Interaction of Hb with Platinum-Containing Anticancer Drugs

The Hb molecule in the blood is one of the target biomolecules that some drugs and their metabolites bind preferentially. Just like environmental toxicants form Hb complexes, these drugs also interact with Hb to form Hb complexes of drugs. A study on

the interaction of Hb with drugs will improve our understanding of the structure and function of Hb and will also provide information about drug action and toxicity.

1.3.1 Platinum-Containing Drugs

Platinum-containing drugs, such as cisplatin and carboplatin, have been widely used in clinical practice as chemotherapeutic agents. Oxaliplatin (Eloxatin^{TM}) is a relatively new third-generation platinum drug that was approved by the U.S. Food and Drug Administration (FDA) in August 2002 to be used in combination with infusional 5-fluorouracil (5-FU) and leucovorin for the treatment of colorectal cancer [17]. Colorectal cancer has been estimated to be the fourth largest cause of cancer deaths [18]. Among thousands of platinum-containing compounds being developed, oxaliplatin is the first platinum-containing drug that demonstrates convincing anticancer activity against colorectal cancer.

1.3.2 Oxaliplatin and Its Transformation Products

The chemical name of oxaliplatin is trans-[(1R,2R)-1,2-cyclohexanediamine-N,N'] [oxalato(2-)-O,O'] platinum (II) (molecular formula $C_8H_{14}N_2O_4Pt$ and molecular mass 397.3 Da). Its chemical structure is shown in Figure 1.3. The platinum atom is complexed with 1,2-diaminocyclohexane (DACH), which is a carrier ligand, and with an oxalato-ligand as a leaving group. Oxaliplatin has a unique DACH group, which makes it different from other platinum drugs with respect to anticancer activity and toxicity profile [19]. The oxalate-ligand in oxaliplatin improves its water solubility.

Oxaliplatin undergoes a rapid and extensive nonenzymatic transformation to form metabolites. There is no evidence that cytochrome P450 is involved in its metabolism *in*

vitro [20]. The transformation reactions are mediated primarily through the displacement of the oxalate group by H_2O and endogenous nucleophiles, such as Cl^- and HCO_3^- ions [21]. A number of platinum-containing derivatives have been observed in plasma ultrafiltrate samples from patients, including monochloro-DACH platinum, dichloro-DACH platinum, and monoaquo- and diaquo-DACH platinum [22]. These species are cytotoxic and can form complexes with amino acids, proteins, and other macromolecules in plasma and tissues [23].

The transformation and distribution of oxaliplatin in rat blood after *in vitro* incubation was investigated by Luo et al. [24,25]. They showed that in rat plasma, the leaving group of oxaliplatin can be displaced by chloride and water; $Pt(DACH)Cl_2$ and $Pt(DACH)(H_2O)_2$ were detected and identified. Furthermore, these species further react with sulphydryl-containing plasma proteins or small nucleophiles such as glutathione, cysteine, and methionine to form Pt-DACH complexes (Figure 1.3). Oxaliplatin is also able to diffuse into the red blood cells of rats. The metabolites, including $Pt(DACH)Cl_2$, $Pt(DACH)(Cys)_2$, and $Pt(DACH)(H_2O)_2$ were identified.

In vivo, oxaliplatin also undergoes extensive transformation in cancer patients. Two hours after the end of infusion, $Pt(DACH)Cl_2$, DACH, and $Pt(DACH)(H_2O)Cl$ complexes can be found in the plasma ultrafiltrate from cancer patients treated with oxaliplatin [26]. The platinum complexes with nucleophile species such as methionine, cysteine, or glutathione were found in the plasma of patients (Figure 1.3). These active species, $Pt(DACH)Cl_2$, $Pt(DACH)(H_2O)Cl$, and $Pt(DACH)(H_2O)_2$, have been shown to be more cytotoxic than oxaliplatin [27,28].

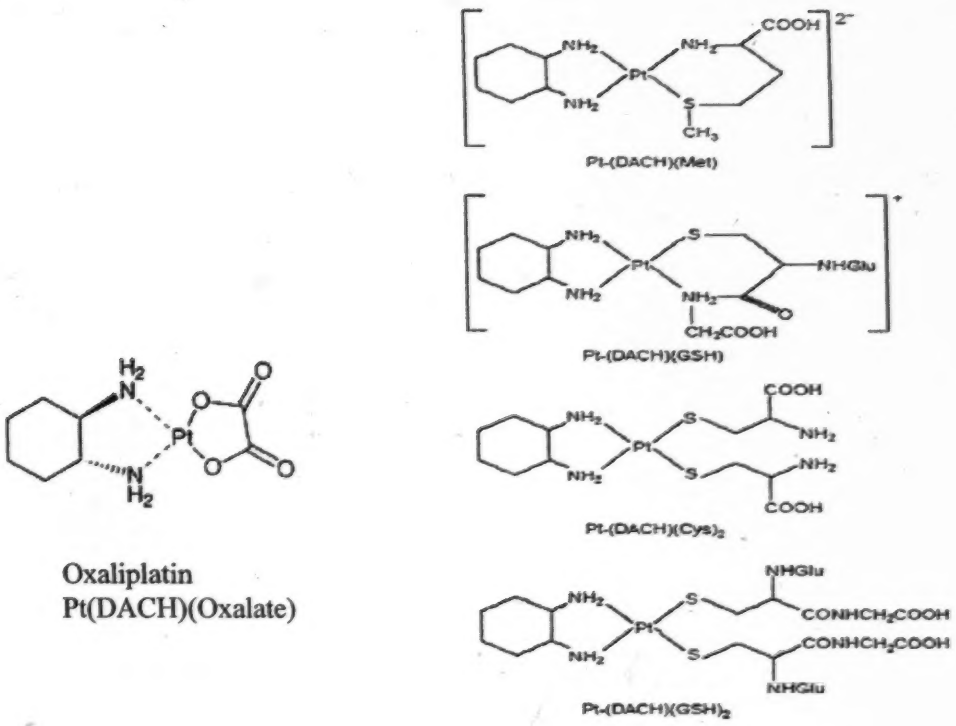

Figure 1.3 Chemical structure of oxaliplatin and its main transformation products.

1.3.3 Pharmacokinetics Study

In vitro platinum drug binding to human plasma was investigated by Pendyala and Creaven [29]. The binding of the platinum in oxaliplatin to plasma was found to be considerable, with 85-88% of the total platinum bound within 5 hours with an average

half-life of 1.71 hour. The binding of oxaliplatin to plasma proteins *in vivo* was investigated in patients receiving 130 mg/m^2 (body surface area) oxaliplatin by a 2-hour infusion every 3 weeks for five cycles. At the end of infusion, the mean percentage of platinum bound to plasma was 65.5% [30].

The platinum in oxaliplatin has also been shown to irreversibly bind to and accumulate in red blood cells [29]. When incubated in whole blood, a significant portion of the total platinum (around 37%) was sequestered into RBC within the first 2 hours; and this fraction was not exchangeable into plasma. *In vivo* studies also showed that platinum accumulated in RBC after oxaliplatin was administered by infusion (130 mg/m^2) over 2 hours every 3 weeks and that its half-life was equivalent to that of RBC [31]. Oxaliplatin's platinum distribution in the blood is distinct from that of cisplatin. Oxaliplatin shows a particular accumulation in RBC while cisplatin does not accumulate much in RBC [32].

1.3.4 Toxicity

Oxaliplatin has a different toxicity profile from cisplatin. The side effects associated with cisplatin are renal toxicity, peripheral motor neuropathy, and emesis [33]. In contrast, the main toxicity associated with oxaliplatin is peripheral sensory neuropathy, which may result in the feeling of numbness or tingling, especially in the hands or feet or around the mouth or throat. Other common side effects of oxaliplatin are vomiting, diarrhea, anemia, increased risk of bleeding or infection, or allergic reaction [17]. With the expanded use of oxaliplatin for the treatment of colorectal cancer, oncologists should be aware of the possibility of these side effects. Several cases have been reported on anemia induced by oxaliplatin treatment [34-37]; this drug-induced hemolytic anemia

may be acute and fatal [34]. To date, the exact mechanism of oxaliplatin-induced hemolytic anemia in these patients is unclear, although Hofheinz et al. proposed two potential mechanisms [35]. One common feature among these cases is the high cumulative dose in RBC after exposure to oxaliplatin. Accumulation of platinum in RBC has been demonstrated in patients over repeated courses of oxaliplatin and Gamelin et al. suggested that it was possibly related to the subsequent anemia [31].

1.3.5 Oxaliplatin-Protein Interactions

It is widely accepted that platinum drugs interact with genomic DNA and form DNA complexes, which are directly responsible for cytotoxic activities. However, there have been few reports on the possible contribution of the protein targets to the cytotoxic effect and side effects of oxaliplatin. Pharmacokinetics in A2780 cells show that the rate of protein binding is high for oxaliplatin [38]. The binding of platinum drugs to cellular proteins via sulphur atoms in the cysteine and methionine residues may affect the activity of some important functional proteins. Therefore, it is postulated that platinum drug binding to proteins may be important for the activity of the drug [39] and may be the likely cause of some of its side effects [40]. Studying the oxaliplatin-hemoglobin interaction will result in more insights into the pharmacokinetics of the drug and provide a better understanding of its mechanism of action and toxicity.

1.4 Conventional Methods for Analysis of Hb and Hb complexes

Hemoglobin is one of the most commonly measured protein molecules in clinical laboratories. It is important to detect and quantify the normal hemoglobin, abnormal hemoglobin and the glycated hemoglobin levels in the blood. Detection of clinically

significant abnormal hemoglobin is helpful for diagnosis of hemoglobinopathy, and the glycated hemoglobin level is used as an excellent indication of the average blood glucose level. Gel Electrophoresis and High Performance Liquid Chromatography with UV detection are two conventional analytical methods for analysis of hemoglobin and hemoglobin complexes.

Hemoglobin electrophoresis is based on the different electrophoretic mobility of normal hemoglobin from other forms of hemoglobin. Hemoglobin electrophoresis can be conducted at alkaline pH (cellulose acetate membrane or alkaline agarose), or at acid pH (citrate agar or acid agarose), or by isoelectric focusing [41-42]. Automated high-performance liquid chromatography is used more and more in clinical laboratories for hemoglobin analysis [43]. The ion-exchange column is used to separate normal hemoglobin from other forms of hemoglobin based on their different ion exchange capability. Although these two conventional methods have been widely used, they still have some limitations. For example, they cannot determine the molecular mass of hemoglobin accurately or characterize the specific form of hemoglobin. As an advanced analytical technique, mass spectrometry has become a widely accepted and increasingly important analytical tool for analysis of proteins, including hemoglobin.

1.5 Mass Spectrometry

Mass spectrometry (MS) is an analytical technique used for measuring the molecular weight (MW) of an analyte. MS has evolved to become an irreplaceable and powerful technique for analysis of large biomolecules, such as protein molecules. The discovery of the electrospray ionization (ESI) [44] and matrix-assisted laser desorption

ionization [45] techniques allows soft ionization of large biomolecules and therefore makes MS a revolutionary analytical tool for analysis of large biomolecules. Dr. John B. Fenn and Dr. Koichi Tanaka shared half of the 2002 Nobel Prize in Chemistry for their contributions to the ESI and soft laser desorption ionization techniques respectively.

MS has become the key technology in the emerging field of proteomics [46]. It can be used to: accurately measure the molecular weight of a protein molecule, identify the protein by peptide mass fingerprinting, analyze the peptide sequence through tandem MS, detect post-translational modifications, such as phosphorylation and glycosylation, and study noncovalent interactions such as intact protein complexes.

Mass spectrometers are composed of three essential parts. The first part is the ion source, which produces gas phase ions from the sample. The second part is the mass analyzer, which resolves ions based on their mass to charge (m/z) ratio. The third part is the ion detector, which detects the ions resolved by the mass analyzer. In short, mass spectrometer converts the components of a mixture to gas phase ions and analyzes them on the basis of their m/z [47].

1.5.1 Electrospray Ionization (ESI)

Electrospray is one of the most commonly used ion sources for analysis of proteins by mass spectrometry. The electrospray process is governed by a number of chemical and physical parameters that together determine the efficiency of ionization [48]. Electrospray is a method that allows the transfer of ions in solution to the gas phase. The analyte solution is passed through a capillary tube held at high electrical potential and the solution emerges as a spray or mist of small charged droplets that go through the desolvation process to produce bare analyte ions into the mass analyzer. The desolvation

process is critically important to generate sufficient bare ions for detection. In some instrument designs, the droplets pass through a heated capillary, which assists the desolvation process [47]. In others, a curtain of nitrogen gas passes across the spray to facilitate desolvation.

Figure 1.4 schematically shows the electrospray ionization of a protein. The protein sample in solution flows through a capillary, to which a high voltage of 3000 V is applied. The protein forms positive ions under acidic pH via protonation of basic groups, such as lysine and arginine. During ESI, protein molecules form multiply charged ions, for instance, charge 5+, charge 6+, and charge 7+. These multiply charged ions are extracted and separated by the mass analyzer based on their mass to charge ratio. A mass spectrum is obtained by recording the ion signals of these multiply charged ions resolved by the mass analyzer. The molecular weight of the protein is obtained from the deconvoluted mass spectrum. An advanced mass spectrometry instrument, such as a hybrid quadrupole time-of-flight, can measure the molecular weight of a protein accurately.

ESI has many advantages: first, it is a "soft" ionization method because the transfer of ions from solution to gas phase imparts negligible internal energy to the analytes. Second, a protein molecule can form multiply charged ions during ESI and therefore the m/z ratio can become small enough to allow a large protein molecule to be analyzed by ordinary mass spectrometers such as quadrupole. Also, the multiply charged ions in the mass spectrum can improve the accuracy of the molecular weight determination. Third, ESI transfers analytes in liquid phase into gas phase ions, making it an excellent interface for coupling online separation techniques like high performance

liquid chromatography and capillary electrophoresis to MS. One notable shortcoming of ESI is its susceptibility to ion suppression effects. When the sample solution contains high salt concentrations (that is, > ~1 mM), the ionization of analytes is hindered.

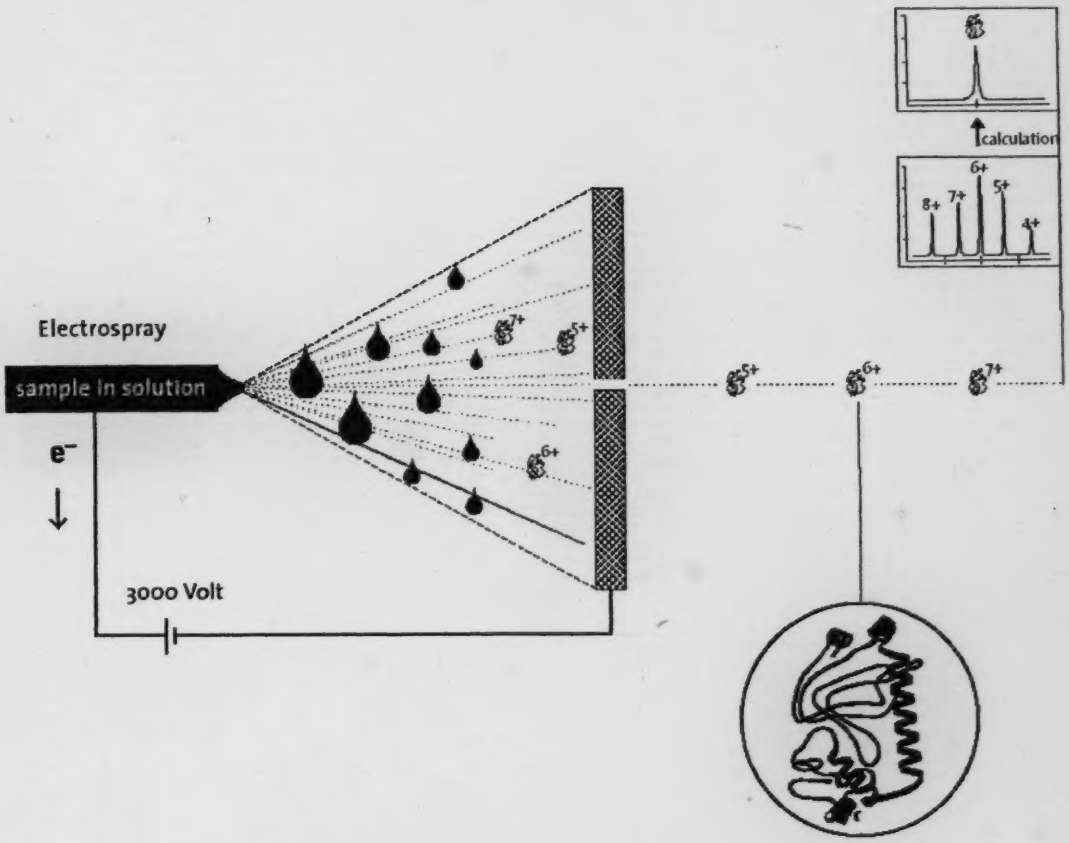

Figure 1.4 Diagram of how ESI-MS analyzes a protein sample.

1.5.2 Nanoelectrospray Ionization

ESI is conventionally performed using large needle dimensions (I.D. range 100 μm to 200 μm) and the sample is sprayed at relatively high flow rates of μL/min. Nanoelectrospray ionization (nanoESI) is essentially a miniaturized version of

conventional ESI. It operates at a very low flow rate of ~ 20 nL/min, with a spraying orifice of 1-2 μm obtained by pulling the nanospray capillary to a fine tip [49].

The major advantages of nanoelectrospray over conventional ESI are: First, there is considerably less sample consumption and better sensitivity. In theory, a few hundred nanoliters of sample are required and in practice, a volume of 1-2 μL is enough to work with. Second, extremely low flow rates can offer increased analysis time, which is suited for ion fragmentation experiments by tandem mass spectrometry. Third, the desolvation process is more efficient owing to the smaller initial size of the droplets and it is possible to spray aqueous samples without organic solvents, which is suitable for maintaining the native structures of protein molecules.

1.5.3 Quadrupole Mass Analyzer

The quadrupole mass analyzer (also appropriately called quadrupole mass filter) is one of the most commonly and routinely used MS instruments. As shown in Figure 1.5, it is composed of four rods arranged as two sets; opposite rods are electrically connected. A combination of direct current (d.c.) voltage and alternating current voltage (a.c.) is applied to each pair of rods to produce a complex, oscillating movement of the ions as they move from the beginning of the mass filter to the end. Ions with a specific m/z have trajectories in the quadrupole mass filter that are stable or resonant and remain in the mass filter, while other ions have unstable or nonresonant trajectories and will strike one of poles and be lost.

The quadrupole can also be set up to contain and transmit ions in a range of m/z by applying a radio frequency r.f.-only field. This use is significant because it allows quadrupoles to function as sophisticated lenses in some regions of instruments.

Depending on the physical parameters of the quadrupole, the upper m/z limit can vary from 650 to 4000; the mass accuracy is generally in the hundreds of ppm [50]. The mass resolution is a function of the ratio of the r.f. and d.c. voltages and typically the unit mass resolution is obtained over the whole mass range.

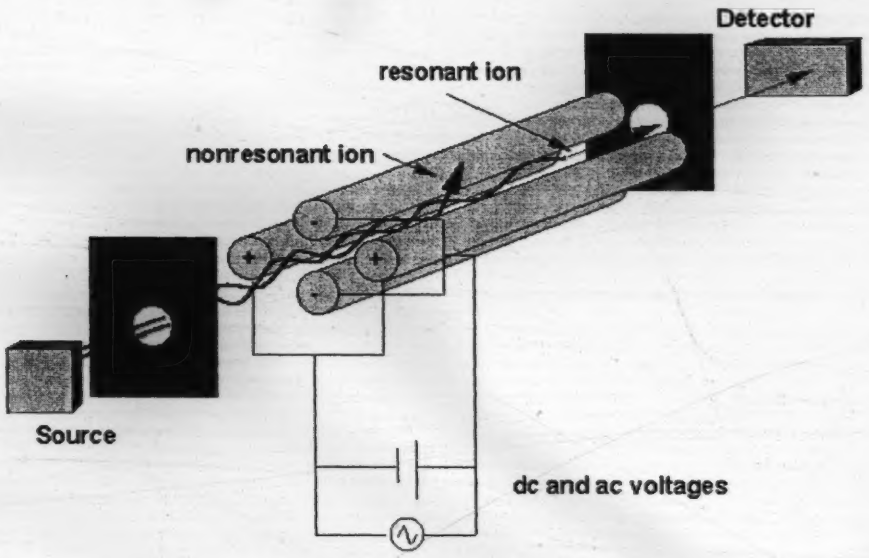

Figure 1.5 Schematic diagram of a quadrupole mass filter.

1.5.4 Time-of-Flight Mass Analyzer

The principle of a time-of-flight (TOF) mass analyzer is elegantly simple. In a linear TOF, ions are extracted from an ion source in short pulses and then directed down an evacuated straight tube to a detector. The time taken to travel the length of the drift or

flight tube depends on the mass of the ions and their charge. The time is related to the square root of m/z. The greater the mass to charge ratio of an ion, the longer time it takes to reach the detector. The linear TOF has a limitation of mass resolution.

Reflectron, an ion mirror, is used to improve the resolving power of TOF. In a reflectron TOF, after traveling through one flight distance, the ions enter an electrostatic mirror that turns the ions around and sends them down a second flight distance to the detector. Since not all ions of any one given m/z value reach the same velocity after acceleration and not all of them are formed at exactly the same point in the ion source, there are some slight differences in the velocities of ions with the same m/z. The function of a reflector is to compensate for small differences in velocities, resulting in improvement of the mass resolution of the TOF mass spectrometer [51].

1.5.5 Hybrid Q-TOF Mass Spectrometer

In order to further improve the performance and additional features of a mass spectrometer, a combination of a quadrupole with a TOF mass analyzer was developed. [52]. A typical hybrid Q-TOF mass spectrometer available now is comprised of three quadrupoles and one reflectron TOF. Figure 1.6 shows the schematic diagram of the instrument structure of Q-TOF (from Applied Biosystems/MDS Sciex). The first quadrupole is called Q0 and is used for collisional cooling and focusing of the ions entering the mass analyser; the second quadrupole Q1 is used as a mass filter; and the third quadrupole Q2 is used as a collision cell. Both Q0 and Q2 are operated in the r.f.-only mode.

For a full scan mass spectrum, the Q-TOF is operated as a single MS using the TOF section. The mass filter Q1 is operated in the r.f.-only mode so that it serves merely as a transmission element, while the reflectron TOF analyzer is used to separate ions.

For tandem MS analysis, Q1 is operated in the mass filter mode to transmit only the parent ion of interest, typically selecting a mass window from 1 to 3 m/z wide depending on the desire to transmit the full isotopic cluster. The ion is then accelerated to an energy of between 20 and 200 eV before it enters the collision cell Q2, where it undergoes collision-activated dissociation (CAD) after the first few collisions with neutral gas molecules (argon or nitrogen) [52]. The TOF section can separate and record the mass spectra of product ions or precursor ions.

One of the key advantages of the hybrid Q-TOF is that it has a high sensitivity and high mass accuracy for both single MS mode and tandem MS mode (precursor ion scan mode or product ion scan mode) because TOF is capable of much higher mass resolution than quadrupole. The TOF used in the QSTAR Q-TOF mass spectrometer (Applied Biosystems/MDS Sciex) has a mass range of 5-12000 m/z and a resolution up to 9000 (FWHM, full peak width at half-maximum) at m/z 800 [53].

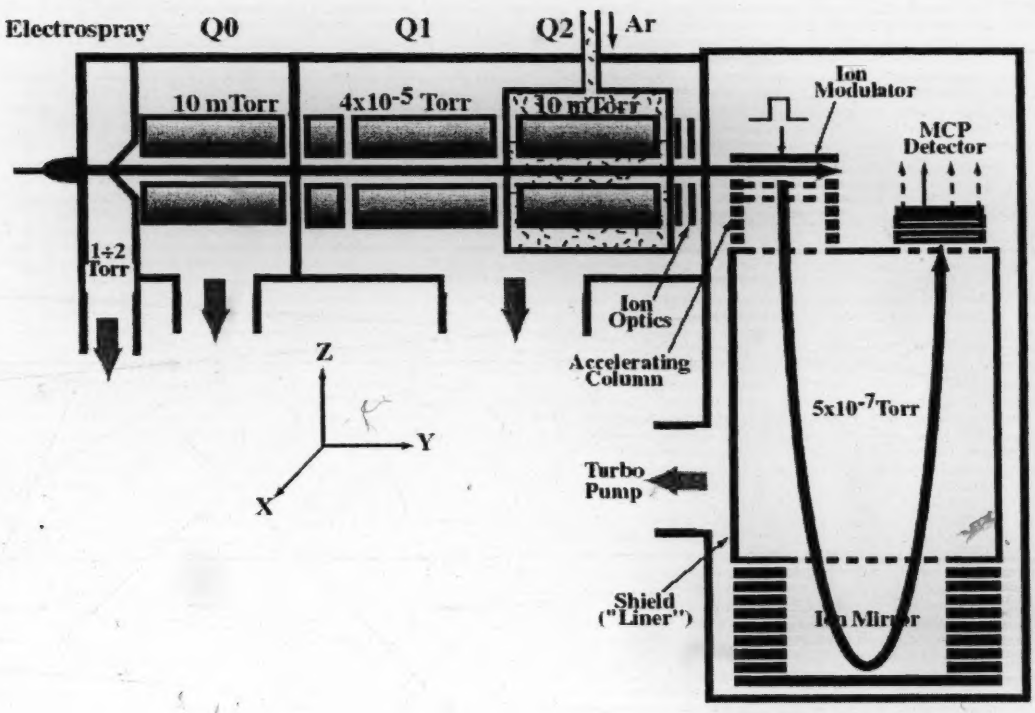

Figure 1.6 Diagram of the quadrupole/time-of-flight mass spectrometer (Applied Biosystems/MDS Sciex).

1.6 Challenges in Analysis of Intact Hb Complexes by MS

Mass spectrometry has already been applied to study the hemoglobin molecule and hemoglobin complex [46]. However, most of these studies were involved in detecting the separate α- polypeptide chain or β- polypeptide chain of the Hb and their complexes rather than the intact Hb and intact Hb complexes. Because the structure of the intact Hb tetramer is closely related to its biological function, it is important to detect the intact Hb tetramer and Hb complexes using MS.

MS has been widely and readily applied to study the primary structure of a protein; however, it is difficult to detect a noncovalent protein complex such as the intact Hb tetramer using MS. The noncovalent protein complex in solution must be transferred to gas phase ions that can be detected by the MS instrument. The efficient generation of intact noncovalent protein complex ions and maintaining these ions without dissociation in the gas phase remain challenging. ESI-MS has demonstrated good utility to detect and study intact noncovalent protein complexes because electrospray is a more gentle ionization method than others [54-56]. However, experimental conditions, including instrumental conditions, should be carefully optimized to detect the noncovalent protein complex using ESI-MS [56].

1.7 Objectives of The Thesis

It is highly desirable to detect the intact hemoglobin tetramer and hemoglobin complex, although there are some challenges to detect them using MS. To address these challenges, the first objective of this thesis was to develop a nanoelectrospray hybrid quadrupole/time-of-flight mass spectrometric method to simultaneously detect the intact hemoglobin tetramer and its complex. Chapter 2 describes in detail the development of

the nanoESI-MS method and its application to the detection of the intact Hb tetramer and its glucose complex. The effects of sample solution composition, sample preparation, and instrumental parameters will be investigated and optimized in order to obtain good quality mass spectra of the intact hemoglobin tetramer and its glucose complex. The hemoglobin-glucose complex, called glycated hemoglobin, is potentially useful as a biomarker for long-term glucose levels in human blood.

The second objective of this thesis was to apply this nanoeletrospray ionization mass spectrometric approach to investigate the interactions between the anticancer drug oxaliplatin and the intact Hb tetramer. Chapter 3 describes the *in vitro* and *in vivo* studies of drug binding with the intact Hb tetramer. For the *in vitro* study, the binding stoichiometry and type of Hb-oxaliplatin complexes were determined. The CAD tandem MS studies of Hb-drug complexes were investigated to further characterize the structure of the Hb-drug complexes. For the *in vivo* study, the Hb-oxaliplatin complexes in the cancer patients' red blood cell samples were detected and characterized and the serum albumin-drug complexes in the patients' plasma samples were also detected.

References

1. Hillman RS, Finch CA. *Red Cell Manual Edition5* F.A.Davis: Philadelphia, 1985.
2. Rai DK, Landin B, Alvelius G, Griffiths J. *Anal. Chem.* 2002; 74: 2097.
3. Matthew HR, Freedland RA, Miesfeld RL. *Biochemistry A Short Course* Wiley-Liss: 1997.
4. http://medweb.bham.ac.uk/bmedsci/bms2/chime/structure/structure.html#anchor259353 retrieved on August 26, 2004.
5. http://www.chemistry.wustl.edu/~edudev/LabTutorials/Hemoglobin/MetalComplexinBlood.html retrieved on August 26, 2004.
6. Dickerson RE, Geis I. *Hemoglobin: structure, function, evolution, and pathology* Benjamin/Cummings: Menlo Park, 1983.
7. Bunn HF, Forget BG. *Hemoglobin: molecular, genetic and clinical aspects* W.B.Saunders: Philadelphia, 1986.
8. Little RR, Goldstein DE. *Anal. Chem.* 1995; 67: 393R.
9. DCCT research group. *N. Engl. J. Med.* 1993; 329: 977.
10. Gabbay KH, Sosenko JM, Banuchi GA, Mininsohn MJ, Fluchiger R. *Diabetes* 1979; 28: 337.
11. Skipper PL, Peng X, Soohoo CK, Tannenbaum SR. *Drug Metab. Rev.* 1994; 26: 111.
12. Poirier MC, Santella RM, Weston A. *Carcinogenesis* 2000; 21: 353.
13. Boogaard PJ. *J. Chromatogr B* 2002; 778: 309.
14. Angerer J, Mannschreck C, Gundel J. *Int. Arch. Occup. Environ. Health* 1997; 70: 365.
15. Jones CR, Beyerbach A, Seffner W, Sabbioni G. *Carcinogenesis* 2003; 24: 779.

16. Swenberg JA, Koc H, Upton PB, Georguieva N, Ranasinghe A, Walker VE, Henderson R. *Chem. Biol. Interact.* 2001; 135-136: 387.

17. FDA News http://www.fda.gov/bbs/topics/NEWS/2002/NEW00825.htm retrieved on August 26, 2004.

18. Grahham J, Muhsin M, Kirkpatrick P. *Nat. Rev. Drug Discov.* 2004; 3: 11.

19. Di Francesco AM, Ruggiero A, Riccardi R. *CMLS Cell. Mole. Life Sci.* 2002; 59: 1914.

20. Brandl J, Brian W. *Sanofi Research Report* No. MIH0034, 1998.

21. Graham MA, Lockwood GF, Greenslade D, Brienza S, Bayssas M, Gamelin E. *Clin. Cancer Res.* 2000; 6: 1205.

22. Allen J, Graham MA, Firth J, Woolfrey S, Greenslade D, Morrison JG, McDougall S, Ross P, Cunningham D. *Proc. Am. Assoc. Cancer Res.* 1998; 39: 159.

23. Allen J, Graham MA, Watson D, Chung D, Tabah-Fisch I, Ross P, Cunningham D. *Sanofi Research Report* No. PKM2983, 1998.

24. Luo FR, Wyrick SD, Chaney SG. *J. Biochem. Mole. Toxicol.* 1999; 13: 159.

25. Luo FR, Yen TY, Wyrick SD, Chaney SG. *J. Chromatogr. B* 1999; 724: 345.

26. Allain P, Heudi O, Cailleux A, Le Bouil A, Larra F, Boisdron- Celle M, Gamelin E. *Drug Metab. Dispos.* 2000; 28: 1379.

27. Luo FR, Wyrick SD, Chaney SG. *Oncol. Res.* 1998; 10: 595.

28. Videhult P, Yachnin J, Jerremalm E, Lewensohn R, Ehrsson H. *Cancer Lett.* 2002; 180: 191.

29. Pendyala L, Creaven PJ. *Cancer Res.* 1999; 53: 5970.

30. Graham MA, Brienza S, Misset JL, Cupissol E, Gamelin E, Allain P. *Sanofi Research Report* No. VAR 3149, 1998.

31. Gamelin E, Be Bouil A, Boisdron-Celle M, Turcant A, Delva R, Cailleux A, Krikorian A, Brienza S, Cvitkovic E, Robert J, Larra F, Allain P. *Clin. Cancer Res.* 1997; 3: 891.

32. Boisdron-Celle M, Lebouil A, Allain P, Gamelin E. *Bull. Cancer* 2001; 88: Spec No: S14.

33. Markman M. *Expert Opin. Drug Saf.* 2003; 2: 597.

34. Desranme J, Broustet H, Darodes de Tailly P, Girard D, Saissy JM. *The Lancet* 1999; 354: 1179.

35. Hofheinz R, Nguyen X, Buchheidt D, Kerowgan M, Hehlmann R, Hochhaus A. *Cancer Chemother. Pharmacol.* 2004; 53: 276.

36. Garufi C, Vaglio S, Brienza S, Conti L, D'Attino RM, Girelli G, Terzoli E. *Annals Oncol.* 2000; 11: 497.

37. Chen VMY, Thrift KM, Morel-Kopp M, Jackson D, Ward CM, Flower R. *Transfusion* 2004; 44: 838.

38. Pendyala L, Kidani Y, Perez R, Wilkes J, Bernacki RJ, Creaven PJ. *Cancer Lett.* 1995; 97: 177.

39. Espinosa E, Feliu J, Zamora P, Baron MJ, Sanchez JJ, Ordonez A, Espinosa J. *Lung Cancer* 1995; 12: 67.

40. Gullo JJ, Litterst CL, Maguire PJ, Silis BJ, Holth DF, Woodley PV. *Cancer Chemother. Pharmacol.* 1980; 5: 21.

41. Wada Y. *J. Chromatogr. B* 2002; 781: 291.

42. Wild BJ, Brain BJ. *Ann. Clin. Biochem.* 2004; 41: 355.

43. Joutovshy A, Hadzi-Nesic J, Nardi MA. *Clin. Chem.* 2004; 50: 1736.

44. Fenn JB, Mann M, Meng CK, Wong SF, Whitehouse CM. *Science* 1989; 246: 64.

45. Karas M, Bachmann D, Bahr U, Hillenkamp F. *Int. J. Mass Spectrom. Ion Process.* 1987; 78: 53.

46. Aebersold R, Mann M. *Nature* 2003; 422: 198.

47. Liebler DC. *Introduction to Proteomics: Tools for the New Biology* Humana Press: Totowa, NJ, 2002.

48. The Royal Swedish Academy of Sciences. Advanced information on the Nobel Prize in Chemistry 2002. http://www.kva.se retrieved on March 20, 2005.

49. Wilm M, Mann M. *Anal. Chem.* 1996; 68: 1.

50. Galish GL, Vachet RW. *Nat. Rev. Drug Discov.* 2003; 2: 140.

51. Herbert CG, Johnstone RA. *Mass Spectrometry Basics* CRC Press: 2002.

52. Chernushevich IV, Loboda AV, Thomson BA. *J. Mass Spectrom.* 2001; 36: 849.

53. Training Manual of Applied Biosystems/MDS Sciex.

54. Loo JA. *Mass Spectrom. Rev.* 1997; 16: 1.

55. Heck AJR, Van den Heuvel RHH. *Mass Spectrom. Rev.* 2004; 23: 368.

56. Loo JA. *Int. J. Mass Spectrom.* 2000; 200: 175.

Chapter 2 Development of A Nanoelectrospray Ionization Mass Spectrometry Method for Detection of Intact Hb Tetramer and Glycated Hb

2.1 Introduction

Human hemoglobin plays a central role in transporting oxygen in the blood to the tissues. In the red blood cells, the quaternary structure of hemoglobin is intimately related to its function [1]. The principal human adult hemoglobin (HbA0) consists of two α- and two β-globin chains. An α-globin chain is made up of 141 amino acids (M_r = 15126.4) and a β-globin chain is made up of 146 amino acids (M_r = 15867.2) [2]. The four globin chains associate into an intact Hb tetramer through weakly-bound noncovalent interactions, such as hydrogen bonding, electrostatic interaction, and hydrophobic interaction. Each Hb molecule has four heme groups, each of which is noncovalently bound to each of the globin chains. In dilute solutions, the Hb tetramer can dissociate reversibly to dimers and further to globin monomers [3].

In the blood, glucose binds irreversibly to hemoglobin molecules. The glucose complexes of Hb that can be formed *in vivo* by glucose binding slowly and nonenzymatically to hemoglobin are referred to as glycated hemoglobin [4]. Since the level of glycated Hb correlates very well to the average glucose concentration in the blood from exposure during preceding two or three months, the measurement of glycated Hb is widely accepted as a valuable biomarker for long-term diabetic control [5,6].

Electrospray ionization mass spectrometry (ESI-MS) is a powerful analytical tool for analysis of large biomolecules, such as proteins. ESI-MS has been successfully used for the identification of hemoglobin variants [2,7], the structural characterization of hemoglobin complexes of environmental toxicants [8-10], and the measurement of

glycated Hb on the separate α- and β-globin chains [11,12]. However, these studies were based on measuring the mass of separate α- and β-globin chains and their variants or the complexes of separate α- and β-globin chains. Because the intact quaternary structure of Hb is predominantly present in red blood cells and is directly related to its function in human blood, it is highly desirable to detect the intact Hb tetramer rather than separate α- and β-globin chains. ESI-MS has already demonstrated its utility in the study of noncovalent complexes, including protein interactions with inhibitors, metal ions, carbohydrates, other proteins, and nucleic acid complexes [13-16]. The observation of the noncovalent quaternary structure of human hemoglobin by ESI-MS was first reported by Smith's group [17] and subsequently the detection of the bovine hemoglobin tetramer using ESI-MS was also reported by other researchers [18,19]. However, their mass spectra showed the broad peaks of Hb tetramer ions and the glycated Hb was unable to be distinguished from the Hb tetramer. To date, there are no reports on the detection of complexes of the intact hemoglobin tetramer using mass spectrometry. The objective of this chapter is to develop a nanoelectrospray hybrid quadrupole time-of-flight mass spectrometric method to simultaneously detect the intact Hb tetramer and glycated Hb.

2.2 Experimental

2.2.1 Materials and Sample Preparation

Human hemoglobin (HbA0) and horse heart myoglobin were purchased from Sigma (St. Louis, MO, USA). The purity of Hb was examined using sodium dodecylsulfate (SDS) polyacrylamide gel electrophoresis and two bands corresponding to the α- and β-chains were detected. Therefore, HbA0 was used as received without further

purification. Water, formic acid, methanol, and ammonium acetate were all of HPLC-grade and were purchased from Fisher Scientific (Fair Lawn, NJ, USA). Microcon YM-10 centrifugal filters (membrane NMWL molecular cut-off 10 KDa, Millipore, Nepean, ON, Canada) were used to desalt the protein sample according to the manufacturer's instruction manual.

2.2.2 Instrumentation

Mass spectrometry experiments were performed using an Applied Biosystems/MDS Sciex QSTAR Pulsar i hybrid quadrupole/time-of-flight (Q-TOF) mass spectrometer (Concord, ON, Canada), equipped with a nanoelectrospray ionization source. Analyte solutions were introduced into the source by nanoES capillaries (long and medium, Protana, Denmark). The mass spectrometer was operated in the positive ion mode. Analyst QS software (Applied Biosystems, Foster City, CA, USA) was used for the spectrum acquisition and data analysis. Igor Pro software (WaveMetrics, Lake Oswego, OR, USA) was used to plot the spectrum.

For the nanoelectrospray ionization, sample loading and tip opening are critical to generate a good spectrum. A sample solution was loaded into a silver-coated borosilicate nanoES capillary. The capillary was arranged on the nanoelectrospray assembly and the fine tip of the capillary was gently tapped on the curtain plate to get a spray orifice. The position of the fine tip was monitored using a CCD camera.

In this work, the full scan MS mode (single MS mode) was used and the mass measurements were performed using the TOF section of the instrument, while Q0, Q1, and Q2 were operated in r.f.-only mode. The collision gas in Q2 was used in the single MS mode. Collision gas pressure was set to different value (CAD 2, 5, and 7) The

performance of the instrument was externally calibrated with myoglobin (M_r = 16951.4). Each mass spectrum was acquired by accumulation of 300 scans to improve the signal-to-noise ratio.

2.3 Results and Discussion

2.3.1 Effect of Sample Solution Composition

Detection of noncovalent association of protein complexes such as the intact Hb tetramer is largely dependent on sample solution conditions and ESI-MS instrument conditions. First of all, the composition of the protein sample solution has a dramatic effect on the detection of the intact Hb tetramer using ESI-MS. The commonly used solution condition for normal ESI-MS analysis of a protein sample is a mixture composed of acids, organic solvents, and water. However, this kind of solution composition is not suitable for maintaining intact noncovalent protein complexes, because the acids or organic solvents can destroy the noncovalent binding and denature the protein complex in the solution. In order to use ESI-MS to detect the intact Hb tetramer, it is essential to choose the sample solution condition that can maintain the Hb tetramer in its native folded state and can obtain efficient desolvation of the charged droplets [15]. Therefore, a volatile buffer such as aqueous ammonium acetate is preferred for ESI-MS analysis because it does not form extensive gas phase complexes with the protein, compared with the phosphate or sulfate buffer [15]. We examined the effects of these two different sample solution compositions on the detection of the intact Hb tetramer.

Figure 2.1 presents the typical nanoESI mass spectrum of 10 μM Hb, which was prepared in (a) the 10% methanol water solution containing 0.01% formic acid (pH 4),

and (b) the 5 mM aqueous ammonium acetate buffer (pH 6.5) without acids or organic solvents. Figure 2.1a clearly demonstrates that the major species of Hb detected in the mass spectrum are the α and β subunit of monomers. No ion signals of dimers (αhβh) or tetramer (αhβh)2 were detected. The heme group was also detected in the high ion abundance. The formic acid and methanol used in the Hb sample solution caused the intact Hb tetramer to dissociate into monomers in the solution; therefore, no intact Hb tetramer was detected when formic acid and methanol were used in the protein solution.

When the Hb (10 μM) was prepared in 5 mM aqueous ammonium acetate buffer without acids or organic solvents, the intact Hb tetramer was detected in the mass spectrum. Figure 2.1b shows the typical nanoESI mass spectrum of 10 μM Hb in 5 mM aqueous ammonium acetate buffer, in which there are 7 major peaks. Peaks 5, 6, and 7, at m/z 3393.6, 3582.2, and 3792.5 respectively, correspond to the tetramer ions with charge states of 19+, 18+, and 17+ (T19+, T18, and T17+). Peaks 3 and 4, at m/z 2480.3 and 2686.8 respectively, correspond to the dimer ions with charge states of 13+ and 12+ (D13+ and D12+). Peaks 1 and 2, at m/z 1750.4 and 1969.1 respectively, correspond to the α subunit of monomers with charge states of 9+ and 8+ (M9+ and M8+). The Hb tetramer ions were the predominant species in Figure 2.1b, while a small amount of ion signals of dimers and monomers were also detected. Aqueous ammonium acetate solution could keep the Hb tetramer intact under non-denaturing conditions; therefore, the intact Hb tetramer was detected using nanoESI-MS. Moreover, the heme group was still attached to hemoglobin: no free heme group was detected in Figure 2.1b. Mass spectra (Figure 2.1 a and b) were obtained using different sample solution compositions while keeping the other experimental conditions the same. Therefore, the sample solution

composition can have a dramatic effect on the detection of the intact Hb tetramer. Organic solvents and formic acid were avoided in our further studies and the 5 mM aqueous ammonium acetate buffer was used to detect and study the intact Hb tetramer.

Table 2.1 summarizes the measured m/z and calculated m/z of the peaks in Figure 2.1b and reports the mass accuracy by comparing the measured values with calculated values. The m/z accuracy of the peaks 5, 6, and 7 (T19+, T18+, and T17+) was 88, 139, and 26 ppm, which facilitated and supported the identification of the ions of the intact Hb tetramer.

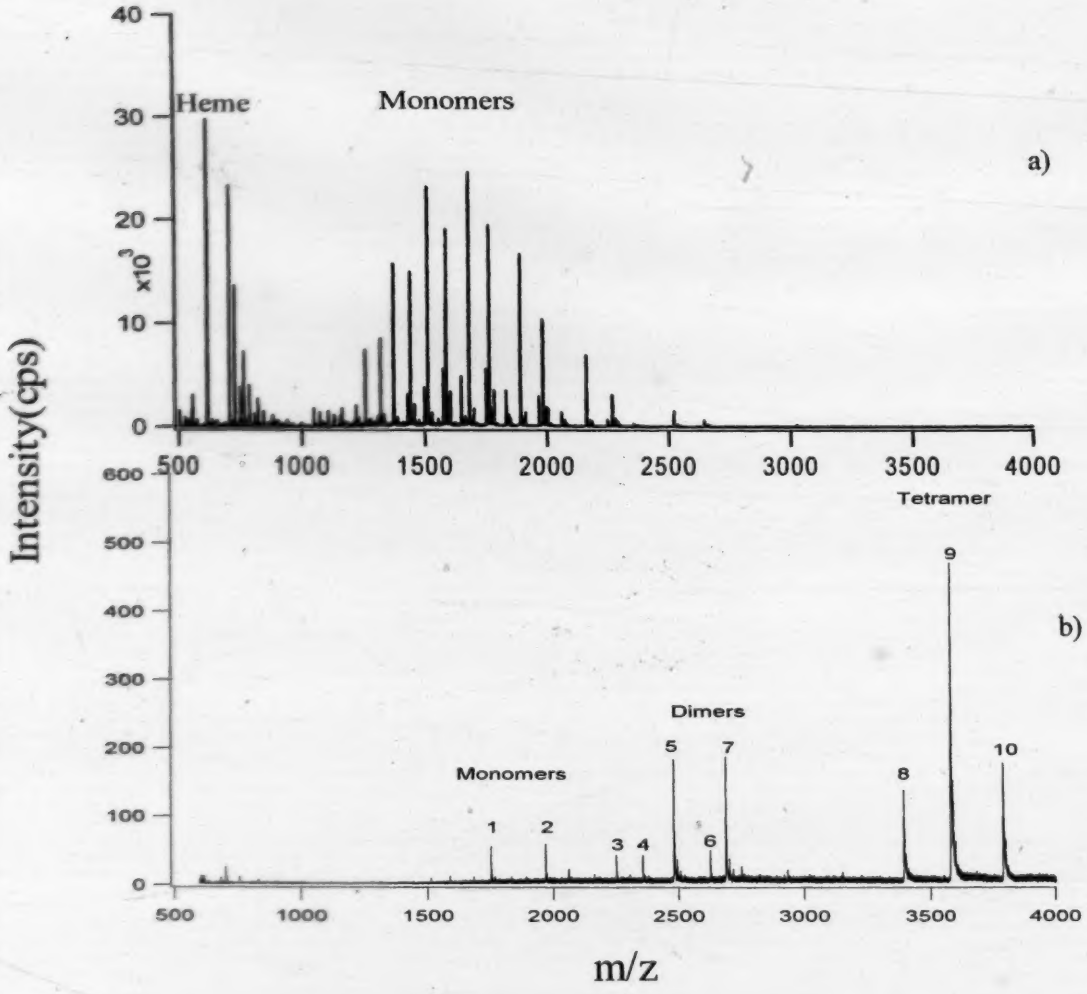

Figure 2.1 Typical nanoESI mass spectrum of 10 μM Hb in: a) 10% methanol solution containing 0.01% formic acid (pH 4), b) 5 mM aqueous ammonium acetate buffer (pH 6.5).

Table 2.1 The measured and calculated m/z of the peaks in Figure 2.1b.

Labelled Peak	Measured m/z	Calculated m/z	m/z Accuracy (ppm)	Identified Peak
Peak 1	1750.4	1750.2	114	M9+ αh 9+
Peak 2	1969.1	1968.9	101	M8+ αh 8+
Peak 3	2250.0	2249.9	44	M7+ αh 7+
Peak 4	2355.9	2355.8	42	M7+ βh 7+
Peak 6	2625.1	2624.8	114	M6+ αh 6+
Peak 5	2480.3	2480.0	121	D13+ αhβh 13+
Peak 7	2686.8	2686.5	112	D12+ αhβh 12+
Peak 8	3393.6	3393.3	88	T19+ (αhβh)2 19+
Peak 9	3582.2	3581.7	139	T18+ (αhβh)2 18+
Peak 10	3792.5	3792.4	26	T17+ (αhβh)2 17+

Footnote: M = monomer, D = dimer, T = tetramer.
αh = heme bound α, βh = heme bound β.

2.3.2 Sample Desalting

ESI-MS analysis of a protein sample is strongly affected by salts, detergents, and other contaminants in the sample solution. It is well-documented that salts and detergents can suppress the ionization of protein analytes [20]. Therefore, it is important to prepare the sample before it is subjected to ESI-MS analysis. There are several ways of desalting protein samples, such as dialysis, size exclusion spin column, and centrifugal filtration [21]. In this study, we chose centrifugal filtration to remove the small molecules from the protein samples.

Figure 2.2 shows the positive nanoESI mass spectra of Hb (10 μM) in 5 mM ammonium acetate buffer a) without desalting, b) after desalting, and c) the small molecule fraction (<10 KDa). The Hb tetramer ion signal was small (Figure 2.2a); however, two predominant ions at m/z 707 and 1049 were detected. It appears that these two ions correspond to the impurities in the solution, which could suppress the ions of the Hb tetramer. The same Hb sample solution was desalted using a Microcon centrifugal filter (molecular weight cut-off 10 KDa). The retentate, which was the fraction of molecular mass more than 10 KDa, was collected and redissolved in aqueous ammonium acetate buffer. Figure 2.2b was a typical nanoESI mass spectrum of the Hb sample in aqueous ammonium acetate after desalting under the same instrumental conditions as Figure 2.2a. The Hb tetramer ions were clearly detected after desalting.

The fraction of the small molecules (less than 10 KDa) was analyzed. Figure 2.2c presents the nanoESI mass spectrum of the filtrate solution after desalting. The ions at m/z 707 and 1049 were detected in the spectrum, confirming that these were impurities in the protein solution. The ions of the impurities caused the suppression of the ions of intact Hb tetramer. This study suggests that sample desalting is essential and makes it easy to detect the intact Hb tetramer using ESI-MS.

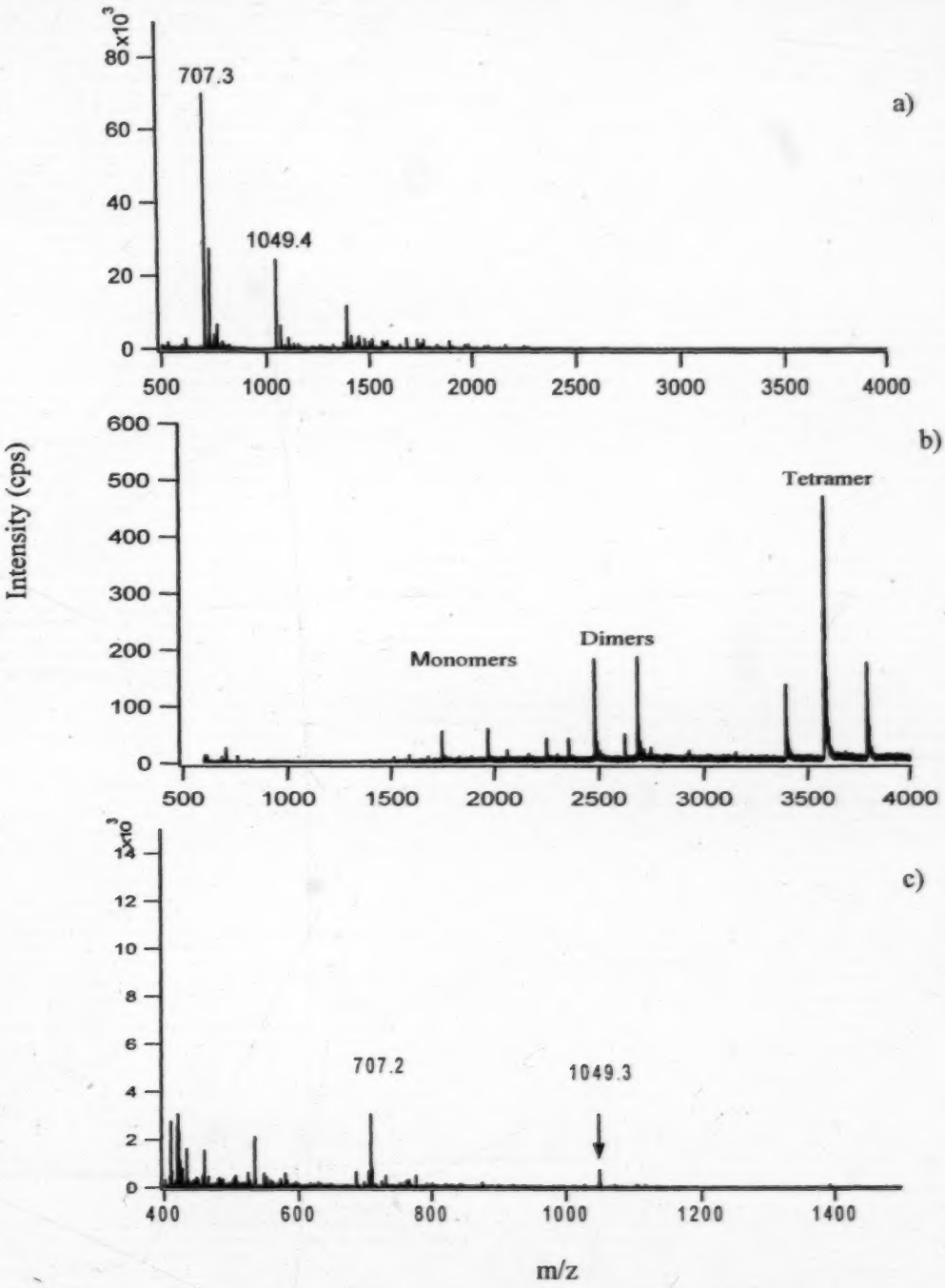

Figure 2.2 a) NanoESI mass spectrum of 10 μM Hb without desalting, b) nanoESI mass spectrum of 10 μM Hb after desalting, c) nanoESI mass spectrum of the filtrate (the fraction of molecular mass less than 10 KDa) using a Microcon YM-10 centrifugal filter.

2.3.3 Effects of Instrumental Parameters on the Detection of the Hb Tetramer

Instrumental parameters must also be carefully evaluated and controlled in order to detect the noncovalent hemoglobin complex using ESI-MS. Different mass spectrometers may have different ESI interface source designs and ion optic paths. For the QSTAR Pulsar i Q-TOF mass spectrometer, several instrumental parameters, including declustering potential, focusing potential, collision gas, and collision energy, were found to be critical for the detection of the intact Hb tetramer. We explored the effects of these instrumental parameters on the detection of the intact Hb tetramer.

2.3.3.1 Effect of Collision Energy

Collision energy (CE) is used to provide energy for selected ions to collide with neutral gas molecules in the collision cell (for MS/MS mode) and also to improve the transmission of ions in the ion optic path (for full scan MS mode). The collision gas was used in this full scan MS mode; therefore, higher CE may cause more fragmentation of the ions in the gas phase. Our purpose is to detect the intact Hb tetramer; therefore, the CE value must be optimized to avoid the fragmentation of the intact Hb tetramer. In this Q-TOF instrument, CE value depends on the Q0 voltage and the RO2 (rod offset on Q2).

Figure 2.3 clearly shows the effect of different CE values on the mass spectrum of the HbA0. Spectra a), b), and c) show the nanoESI mass spectra of Hb sample at a CE value of 11, 4, and 3 eV, respectively, while other instrumental parameters were kept constant. At the CE value of 11 eV, the monomers (peaks M9+ and M8+), dimers (peaks D13+ and D12+), and tetramer (peaks T19+, T18+, and T17+) were detected in Figure 2.3a; however, the relative ion signal of the Hb tetramer was very low. When the CE

value was reduced to 4 eV, the relative ion signal of the Hb tetramer increased (Figure 2.3b). When the CE value was further reduced to 3 eV, the relative ion signal intensities of the tetramer ions (peaks T19+, T18+ and T17+) were greatly increased and the ion signals of the tetramer were present as the predominant species in Figure 2.3c. However, further reducing the CE value reduced the quality of the mass spectrum due to insufficient ion transmission through the ion optic path. Thus, a CE value of 3 eV was used in our study.

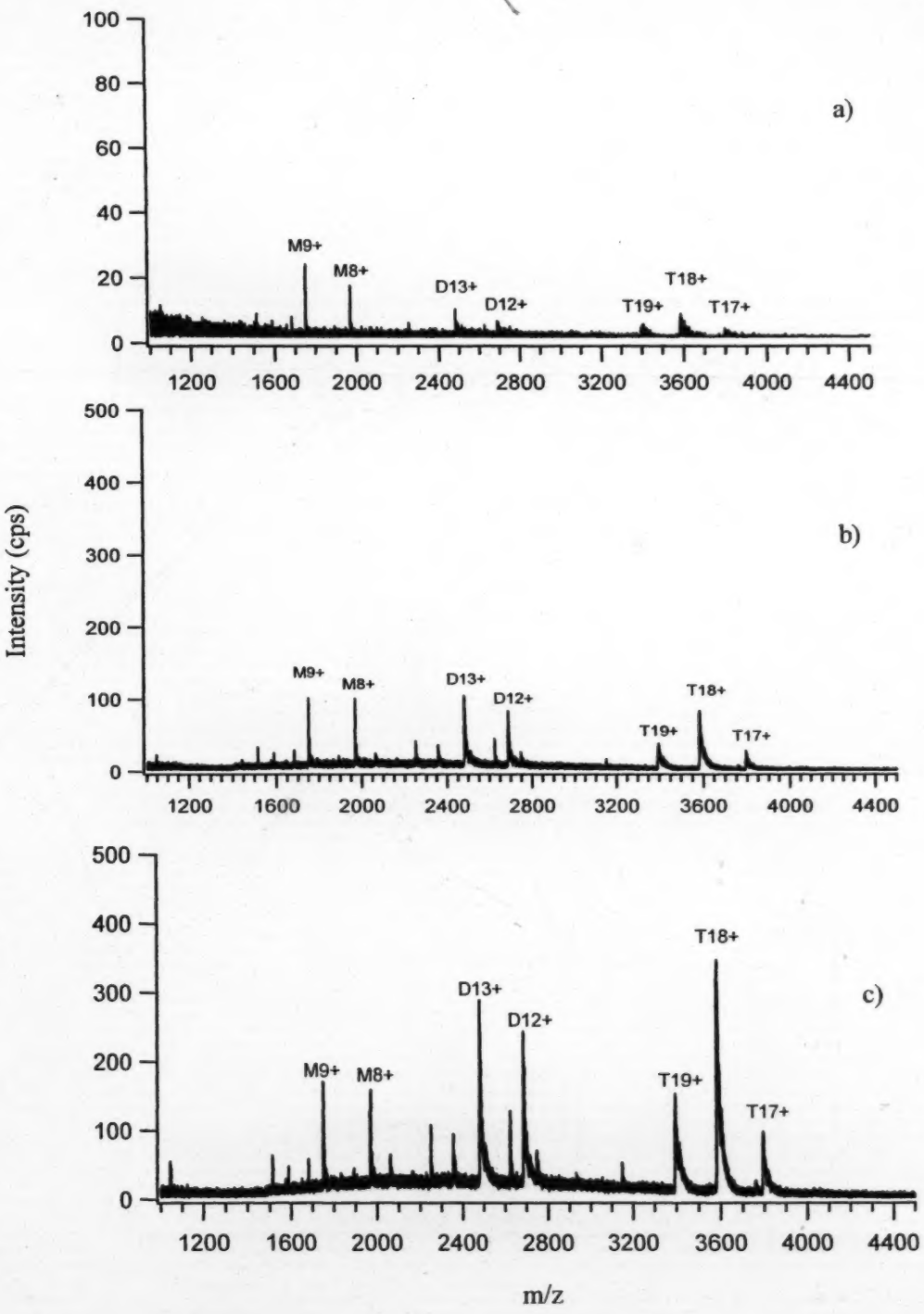

Figure 2.3 NanoESI mass spectrum of 10 μM Hb in 5 mM ammonium acetate buffer using three different CE values: a) CE 11 eV, b) CE 4 eV, c) CE 3 eV. T = Hb tetramer; D = Hb dimer; M = Hb monomer

2.3.3.2 Effect of Declustering Potential and Focusing Potential

The declustering potential (DP) is the difference between the orifice voltage and the skimmer voltage. The higher the potential difference, the greater the amount of declustering or fragmentation. The focusing potential (FP) is the difference between the ring potential and the skimmer potential. Both DP and FP values affect declustering or fragmentation. The DP and FP values should be set high enough to reduce the chemical noise but low enough to avoid fragmentation. Our instrument has DP1 and DP2 settings; however, DP2 had minimal effect on detection of the Hb tetramer relative to DP1. Thus, DP2 was kept constant at the value of 15 V. In this study, we changed the DP1 and FP values at the same time to examine the effect on the detection of the Hb tetramer. The raw mass spectrum was transformed to the deconvoluted mass spectrum so that the multi-charged ion peaks could be mathematically converted into a single molecular mass peak, thus making the raw mass spectrum simpler and easier to identify the species. Figure 2.4 shows the three deconvoluted mass spectra obtained using different DP1 and FP values. When DP1 was at 65 and FP at 215, the tetramer of hemoglobin (αhβh)2 dissociated into dimers (αhβh) (Figure 2.4a). In addition, 2α, 3α, 4α complexes and 2β, 3β, 4β complexes were also detected in Figure 2.4a. It is noteworthy that trimer species like ααβ or αββ were observed in the gas phase using harsher source conditions in other instruments (equivalent to higher DP1 and FP values in our instrument) in the earlier studies [17, 19], while 3α and 3β species were observed in the gas phase in our studies. Although different species were observed in different studies, there was no evidence for the existence of these species in the solution phase, which suggests that they resulted from the random gas phase dissociation of the tetrameric complex [22]. When DP1 was

decreased to 45 and FP decreased to 180, there was less fragmentation. Peaks 4α, 4β disappeared and peaks 2α, 3α, and 3β were detected in Figure 2.4b, and the relative intensity of peaks 2α, 3α, and 3β had decreased. When DP1 was lowered to 30 and FP to 150, the tetramer (αhβh)2 was the predominant species and dimer (αhβh) were also detected in Figure 2.4c. No random aggregates like 2α, 3α were detected in the spectrum, which meant that there was no noticeable dissociation of the tetramer in the gas phase. Therefore, keeping the DP1 value at 30 and the FP value at 150 avoids the dissociation of the Hb tetramer and ensures the good quality of the mass spectrum of the Hb tetramer.

Table 2.2 summarizes the measured mass, calculated mass, and mass accuracy of different species detected in Figure 2.4 at different DP1 and FP. The mass accuracies were within the 108 ppm, which made easy the identification of different Hb species with confidence.

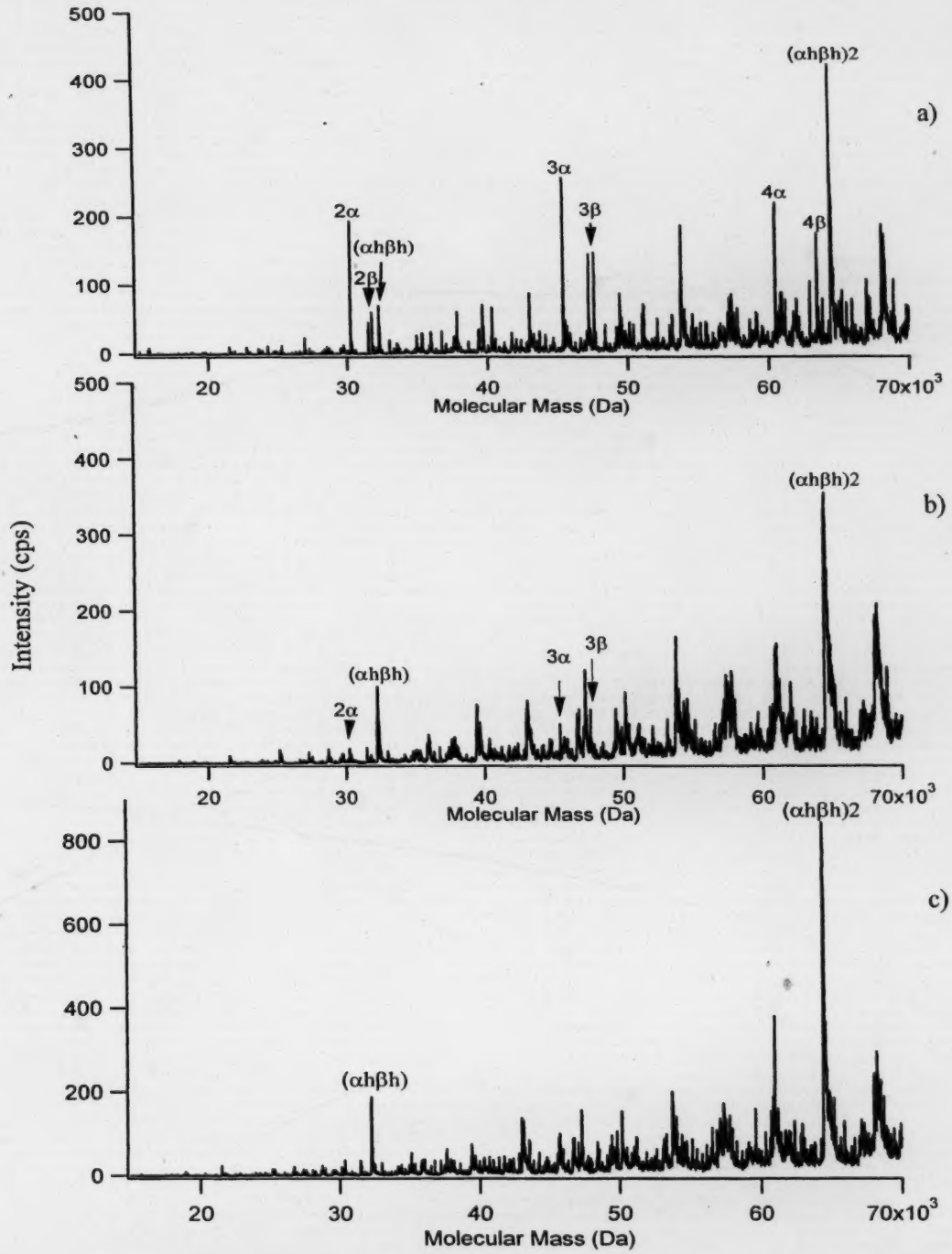

Figure 2.4 Deconvoluted mass spectrum of 10 μM Hb in 5 mM ammonium acetate using three different DP1 and FP values: a) DP1 65, FP 215; b) DP1 45, FP 180; c) DP1 30, FP 150. (αhβh)2 represents the intact heme-bound tetramer; (αhβh) represents the heme-bound dimer; α, β represent the α-globin chain and β-globin chain, respectively.

Table 2.2 Measured mass, calculated mass and mass accuracy for different Hb species detected at different DP1 and FP values.

DP1 FP setting	Measured Mass (Da)	Calculated Mass (Da)	Mass Accuracy (ppm)	Identified Species
DP1 30	64459	64453	93	(αhβh)2
FP 150	32229	32227	62	αhβh
DP1 45	64459	64453	93	(αhβh)2
FP 180	47602	47602	0	3β
	45381	45379	44	3α
	32229	32227	62	αhβh
	30254	30253	33	2α
DP1 65	64460	64453	108	(αhβh)2
FP 215	63469	63468	16	4β
	60510	60506	66	4α
	47604	47602	84	3β
	45382	45379	66	3α
	32230	32227	93	αhβh
	31736	31734	63	2β
	30254	30253	33	2α

2.3.3.3 Effect of Collision Gas

Nitrogen is used as the collision gas (CAD) to provide the neutral gas source into collision cell Q2 when operating MS/MS mode. However, the collision gas in Q2 can also be used in full scan MS mode. Collisional focusing is a patented technique that improves ion transmission in Q0 and Q2 [23]. So ions can be focused in Q0 using elevated pressure to improve transmission into Q1 and collision gas is on at all times for collisional focusing in Q2. We explored the effect of collision gas pressure on the detection of the intact Hb tetramer. Figure 2.5 shows the mass spectra of 10 μM Hb in 5 mM aqueous ammonium acetate buffer using different CAD values of 2, 5, and 7. When CAD was set to 2, the three Hb tetramer peaks T19+, T18+, and T17+ and also the two dimer peaks D13+ and D12+ were the predominant peaks in Figure 2.5a. When CAD was increased to 5, the T19+, T18+, and T17+ peaks became predominant compared with the dimer peaks D13+ and D12+. When CAD was increased to 7, the ion signals of T19+, T18+, and T17+ were greatly improved and it was obvious that the Hb tetramer was the predominant species in Figure 2.5c. These results demonstrate that increasing the CAD value can greatly enhance the transmission of the Hb tetramer, resulting in improved sensitivity and resolution from the additional collisional focusing in the pressurized collision cell [24]. Other researchers also reported that increasing the pressure in the ESI interface and downstream prior to the detector greatly aids in the detection of other noncovalent protein complexes [25-27]. This finding is crucially important for detection of the intact Hb tetramer with improved signal-to-noise ratio and mass resolution, therefore making it possible to simultaneously detect the intact Hb tetramer and its complexes.

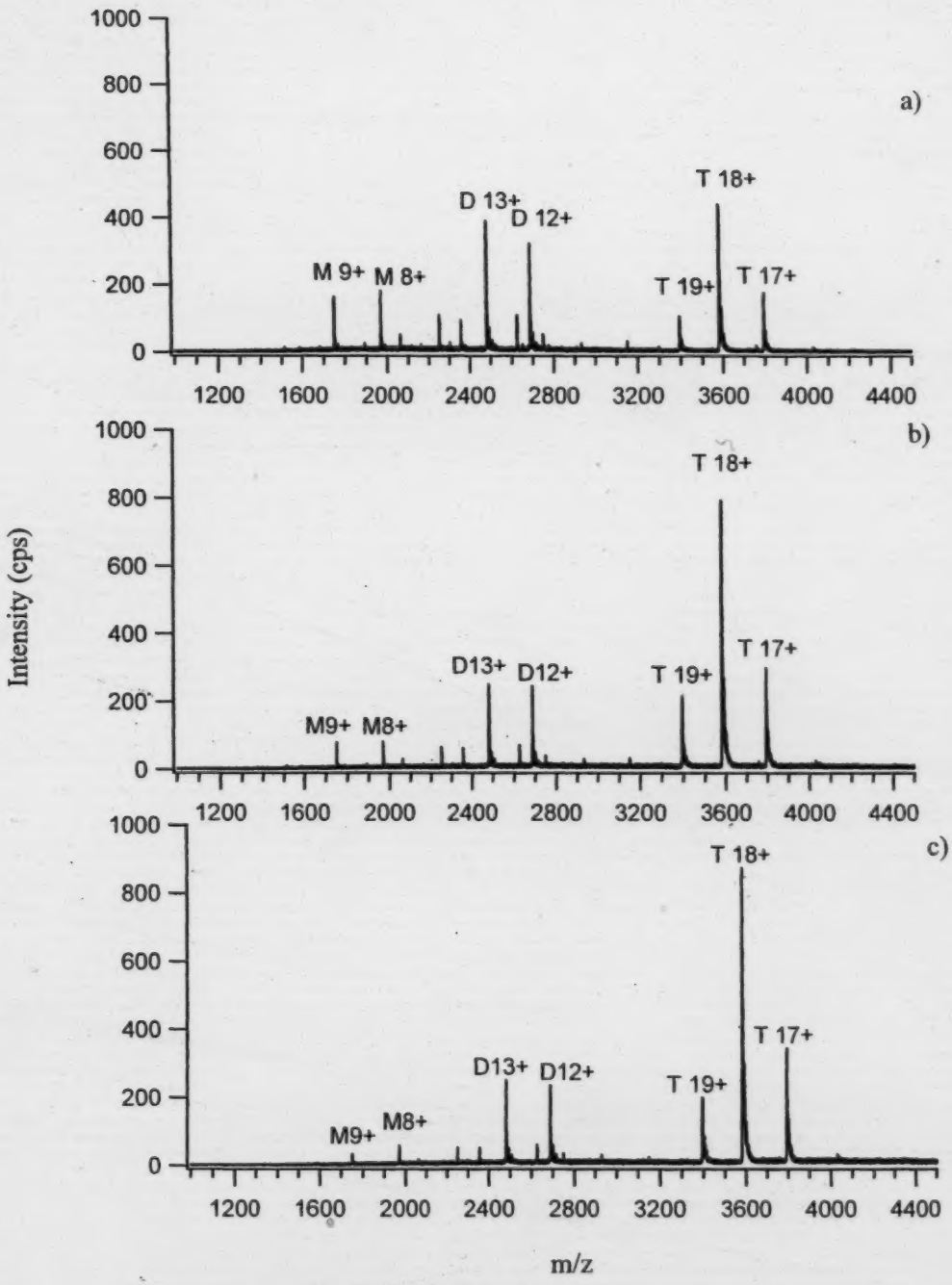

Figure 2.5 Mass spectra of 10 μM Hb in 5 mM ammonium acetate buffer using different CAD values: a) CAD 2, b) CAD 5, c) CAD 7.
T = Hb tetramer; D = Hb dimer; M = Hb monomer

2.3.4 Detection of the Intact Hb Tetramer and Glycated Hb

After optimizing the sample solution condition, desalting the protein sample, and carefully controlling the instrumental parameters, the detection of intact Hb tetramer was obtained by nanoelectrospray Q-TOF mass spectrometry. The technique provides high resolving power, which makes it possible to distinguish the hemoglobin tetramer from its glucose complexes.

Figure 2.6 showed a) the raw mass spectrum of 10 μM Hb tetramer in the mass range 3300-3900 m/z and b) the deconvoluted mass spectrum under optimal experimental conditions. Figure 2.6a showed that there was one additional peak besides each of the three distinctive peaks of the Hb tetramer at m/z 3393.7, 3582.2, and 3792.7 (charge state 19+, 18+, and 17+ ions). The deconvoluted mass spectrum in Figure 2.6b showed that the mass difference between HbA0 (64460 Da) and this additional compound (64622 Da) was 162 Da. The mass difference was very close to the molecular weight of dehydrated glucose (i.e. glucose-H_2O 180-18). As mentioned earlier, glucose in the blood can attach to the hemoglobin by post-translational modification to form the glycated Hb species, which has a mass increment of 162 Da (molecular weight of glucose 180-H_2O 18). Thus the additional peak was identified as the glycated Hb species. The calculated and measured molecular mass of HbA0 and glycated Hb are shown in Table 2.3. The calculated molecular mass of the HbA0 tetramer is 64453 Da, which is obtained by adding the mass of two α-globin chains, two β-globin chains, and four heme groups. The calculated molecular mass of glycated Hb is 64615 Da (64453 plus 162). The mass accuracy achieved was approximately 100 ppm and was quite satisfactory given the relatively high molecular mass of the Hb tetramer.

Glycated forms of the α-globin chain and β-globin chain of Hb were studied by Roberts et al. using the ESI-MS method [11] and by Lapolla et al. using the MALDI-TOF method [28]. Their studies revealed that glycation can occur in both the α-globin and β-globin chain and that one glucose molecule was attached to each of α-globin chain and β-globin chain. The primary form of glycated Hb is HbA1c, which is defined as one stable glucose bound to the N-terminal valine residue of the β-globin chain. It was unexpected to detect both glycated α-globin chain and glycated β-globin chain from their experiments. We report here the detection of the glucose complex to the intact Hb tetramer for the first time. Our studies found that the major glycated Hb species was one glucose molecule bound to each intact Hb tetramer molecule. These results are consistent with existing knowledge about the glycated Hb. However, further study is needed to characterize the structure of this glycated species and there is other species needed to be identified in the spectrum.

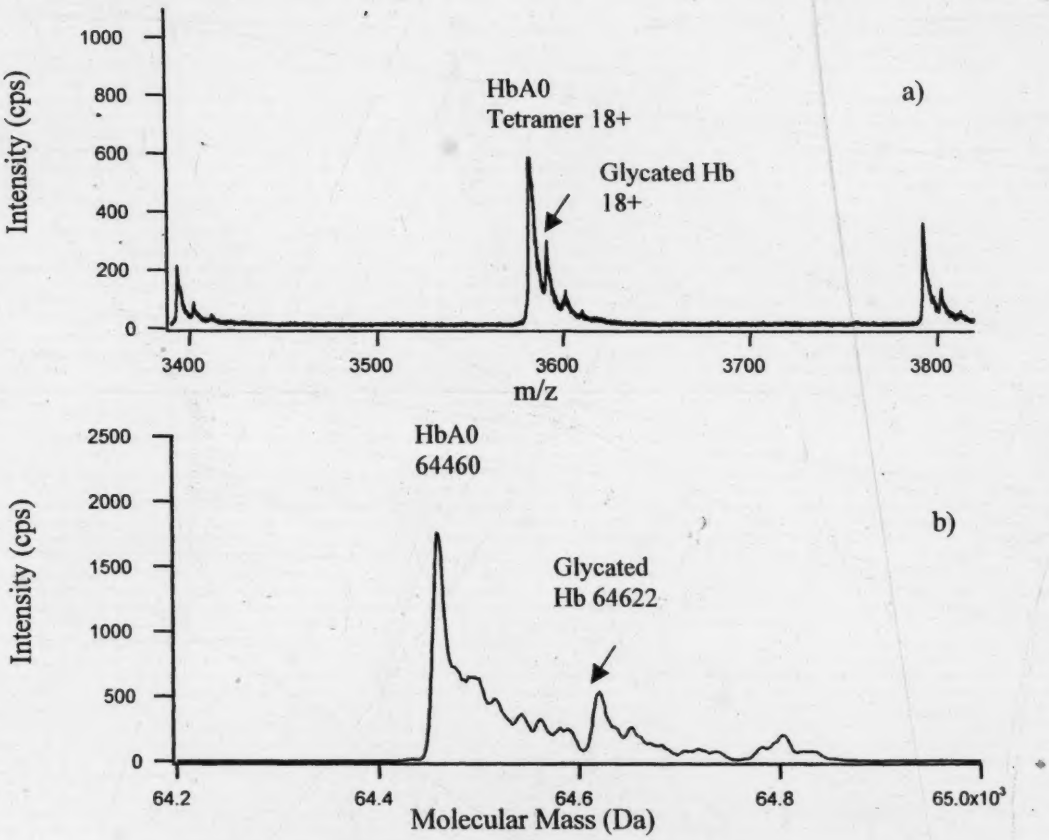

Figure 2.6 a) NanoESI mass spectrum of 10 μM HbA0 in 5 mM aqueous ammonium acetate buffer in the mass range 3300-3900 m/z; b) deconvoluted mass spectrum of HbA0 and glycated Hb.

Table 2.3 Calculated and measured molecular mass of HbA0 and glycated Hb

Species	Calculated Values	Experimental Values					
	Molecular Mass (Da)	19+ (m/z)	18+ (m/z)	17+ (m/z)	Molecular Mass (Da)	Mass difference (Da)	Mass accuracy (ppm)
HbA0	64453	3393.7	3582.2	3792.7	64460	7	104
Glycated Hb	64615	3402.1	3591.0	3799.1	64622	7	104

Note: the calculated mass of glucose minus water is 162.1.

References

1. Matthew HR, Freedland RA, Miesfeld RL. *Biochemistry A Short Course* Wiley-Liss: 1997.
2. Rai DK, Landin B, Alvelius G, Griffiths J. *Anal. Chem.* 2002; 74: 2097.
3. Riggs A. *Methods Enzymol.* 1981; 76: 5.
4. Little RR, Goldstein DE. *Anal. Chem.* 1995; 67: 393R.
5. DCCT research group. *N. Engl. J. Med.* 1993; 329: 977.
6. Gabbay KH, Sosenko JM, Banuchi GA, Mininsohn MJ, Fluchiger R. *Diabetes* 1979; 28: 337.
7. Rai DK, Alvelius G, Landin B, Griffiths WJ. *Rapid Commun. Mass Spectrom.* 2000; 14: 1184.
8. Basile A, Ferranti P, Mamone G, Manco I, Pocsfalvi G, Malorni A, Acampora A, Sannolo N. *Rapid Commun. Mass Spectrom.* 2002; 16: 871.
9. Kristiansson MH, Jonsson BAG, Lindh CH. *Chem. Res. Toxicol.* 2002; 15: 562.
10. Badghisi H, Liebler DC. *Chem. Res. Toxicol.* 2002; 15: 799.
11. Roberts NB, Green BN, Morris M. *Clin. Chem.* 1997; 43: 771.
12. Peterson KP, Pavlovich JG, Goldstein D, Little R, England J, Peterson CM. *Clin. Chem.* 1998; 44: 1951.
13. Smith RD, Light-Wahl KJ. *Biol. Mass. Spectrom.* 1993; 22: 493.
14. Loo JA. *Mass Spectrom. Rev.* 1997; 16: 1.
15. Loo JA. *Int. J. Mass Spectrom.* 2000; 200: 175.
16. Pramanik BN, Bartner PL, Mirza UA, Liu YH, Ganguly AK. *J. Mass Spectrom.* 1998; 33: 911.

17. Light-Wahl KJ, Schwartz BL, Smith RD. *J. Am. Chem. Soc.* 1994; 116: 5271.

18. Schmidt A, Karas M. *J. Am. Soc. Mass Spectrom.* 2001; 12: 1092.

19. Griffith WP, Kaltashov IA. *Biochemistry* 2003; 42: 10024.

20. Hill TJ, Lafitte D, Derrick PJ. *Electrospray Ionization Mass Spectrometry* in *Protein-ligand Interactions, Structure and Spectroscopy: a Practical Approach* Harding SE and Chowdhry BZ (Ed). Oxfard University Press: 2001.

21. Chapman JR. *Mass Spectrometry of Protein and Peptides* Humana Press: Totowa, NJ, 2000.

22. Loo JA, Ogorzalek Loo R, Andrews PC. *Org. Mass. Spectrom.* 1993; 28: 1640.

23. Training manual of manufacturer Applied Biosystems/MDS Sciex.

24. Chernushevich IV, Loboda AV, Thomson BA. *J. Mass Spectrom.* 2001; 36: 849.

25. Douglas DJ, French JB. *J. Am. Soc. Mass Spectrom.* 1992; 2: 398.

26. Krutchinsky AN, Chernushevich IV, Spicer VL, Ens W, Standing KG. *J. Am. Soc. Mass. Spectrom.* 1998; 9: 569.

27. Tito MA, Tars K, Valegard K, Hajdu J, Robinson CV. *J. Am. Chem. Soc.* 2000; 122: 3550.

28. Lapolla A, Fedele D, Aronica R, Garbeglio M, Daopaos M, Plebani M, Seragalia R, Traldi P. *Rapid Commun. Mass Spectrom.* 1997; 11: 613.

Chapter 3 Mass Spectrometric Study of Interaction Between Intact Hemoglobin and Oxaliplatin

3.1 Introduction

We successfully developed a nanoESI-MS method to detect the intact Hb tetramer and glycated Hb, described in Chapter 2. In this chapter, we further demonstrate the application of this technique to the study of intact Hb tetramer-drug complexes. Pt-containing drugs have been widely used as chemotherapeutic agents. Oxaliplatin, a relatively new platinum drug, has been used for the treatment of colorectal cancer [1]. Oxaliplatin was chosen as the model compound for this study.

Oxaliplatin (M.W. = 397.3) is an organoplatin complex in which the platinum atom (Pt) is complexed with 1,2-diaminocyclohexane (DACH) and with an oxalate ligand as a leaving group. Pt(DACH)(Oxalate) is used to represent the chemical structure of oxaliplatin. It is widely accepted that platinum drugs, including oxaliplatin, interact with DNA to form Pt-DNA complexes, which are responsible for the drug's cytotoxicity [2-5]. Oxaliplatin can also interact with proteins and it has been postulated that the interaction of platinum drugs with proteins may be related to the activity and side effects of drugs [6,7]. *In vitro* and *in vivo* studies showed that oxaliplatin binds to plasma proteins, and platinum accumulated in red blood cells (RBCs) [8-10]. Gamelin et al. suggested that the accumulation of Pt in RBCs could be possibly related to subsequent anemia [10]. However, the binding of oxaliplatin to proteins has not been adequately characterized. We hypothesize that oxaliplatin accumulates in RBCs through binding to hemoglobin, the main intracellular protein of RBCs. Information about the interaction of oxaliplatin with

the intact Hb tetramer will contribute to a better understanding of how Pt accumulates in the RBCs and may also help us gain some insights on drug toxicity.

There are a number of conventional analytical techniques employed to study the binding of platinum drugs to protein, such as inductively coupled plasma mass spectrometry (ICP-MS) [10], capillary electrophoresis [11], UV spectroscopy [12], and nuclear magnetic resonance (NMR) [13]. However, these methods do not provide high resolution information about the molecular mass of protein and drug-protein complexes. Electrospray ionization mass spectrometry (ESI-MS) emerges as a powerful tool to study platinum-protein complexes and has been employed to study platinum drugs binding with ubiquitin [14], myoglobin [15], and transferrin [16]. However, there is no mass spectrometric study of characterization of the interaction between intact noncovalent protein complexes, such as hemoglobin, and platinum drugs. In this chapter, we will apply the nanoESI-MS method to study the interactions between the intact hemoglobin tetramer and the platinum drug oxaliplatin both *in vitro* and *in vivo*. We will also extend this methodology to examine the human serum albumin-oxaliplatin complexes formed *in vivo*.

3.2 Experimental

3.2.1 Materials

A stock solution (5 mM) of oxaliplatin (99.999%, Sigma-Aldrich, St. Louis, MO, USA) was prepared by dissolving the appropriate quantities of this platinum-containing drug in deionized water. Human hemoglobin (HbA0) and horse heart myoglobin were purchased from Sigma (St. Louis, MO, USA). Hb and myoglobin were used as received

without further purification. All stock solutions were stored at 4 °C in the dark. Formic acid, methanol, ammonium acetate, and deionized water (all HPLC grade) were purchased from Fisher Scientific Company (Fair Lawn, NJ, USA).

Microcon YM-10 centrifugal filters (membrane NMWL, molecular cut-off 10 KDa, Millipore, Nepean, ON, Canada) were used to desalt the protein samples according to the manufacturer's instruction manual.

3.2.2 Instrumentation

NanoESI-MS experiments were performed using a QSTAR Pulsar i hybrid quadrupole/time-of-flight (Q-TOF) mass spectrometer (Applied Biosystems/MDS Sciex, Concord, ON, Canada), equipped with a nanoESI ion source. Analyte solutions were introduced into the source by nanoES capillaries (long and medium, Protana, Denmark). The mass spectrometer was operated in the positive ion mode for detection of the intact hemoglobin and its drug complexes. The samples were desalted using Microcon YM-10 centrifugal filters and were redissolved in 5 mM aqueous ammonia acetate buffer prior to nanoESI-MS analysis. The Analyst QS software (Applied Biosystems, Foster City, CA, USA) was used for the spectrum acquisition and deconvolution of raw mass spectra. Igor Pro software (WaveMetrics, Lake Oswego, OR, USA) was used to plot the spectra.

For the nanoESI ion source, sample loading and capillary opening are critical to acquire good quality spectra. Sample solutions were loaded into silver-coated borosilicate nanoES capillaries. The capillary was installed on the nanoESI assembly and the fine tip of the capillary was gently tapped on the curtain plate to get a fine spray orifice. The position of the fine tip was optimized and monitored using a CCD camera. Mass spectra were acquired with an electrospray voltage of 1100 V.

In the full scan MS mode, mass measurements were performed using the TOF section of the instrument, while quadrupoles Q1 and Q2 were operated in r.f.-only mode. The performance of the instrument was externally calibrated with myoglobin. The instrumental parameters including the declustering potential 1 (DP1), focusing potential (FP), collision gas (CAD), and collision energy (CE) were optimized according to the procedure described in Chapter 2. They were set as follows: DP1 at 30, FP at 150, CAD at 7, and collision energy at 3.

In the tandem MS mode, precursor ions were selected by Q1 using a low resolution window and fragmented in the collision cell Q2. Product ion mass spectra were acquired by collision-activated dissociation (CAD) with a certain collision energy and a collision gas setting.

3.2.3 Methods

3.2.3.1 In vitro Incubation of Oxaliplatin with Hb

A constant concentration of HbA0 solution (10 μM) was mixed with various concentrations of oxaliplatin to obtain oxaliplatin:Hb molar ratios of 1:1, 5:1, and 10:1. Higher concentrations of oxaliplatin were used in this study to enhance the formation of Hb-drug complexes. These mixtures were incubated at 37 °C for 24 hours and for 5 days. Parallel incubation of the hemoglobin solution without the drug was used as a control.

For nanoESI-MS analysis, aliquots of 400 μL reaction mixture were desalted using Microcon YM-10 centrifugal filters. The retained residue was redissolved in 5 mM aqueous ammonium acetate buffer and were analyzed for the Hb tetramer-oxaliplatin complexes using positive ionization nanoESI-MS.

3.2.3.2 Red Blood Cell Lysis Methods

Freezing/thawing method

The whole blood samples from the normal human adult control were collected in heparin-lithium coated tubes. All samples were spun in a centrifuge at 3000 rpm for 15 minutes. The supernatant and the buffy coat were removed. The plasma layer was separated from the RBC layer. The RBC and plasma were separately stored in cryovials and at –35 °C. For analysis, frozen RBCs were thawed on ice. The RBC hemolysate samples were diluted 200-fold with 5 mM aqueous ammonium acetate buffer and desalted using the Microcon YM-10 centrifugal filters prior to nanoESI-MS analysis.

Hypotonic solution method

In this method, cytoplasm of RBC was extracted using a hypotonic solution. First, RBCs were washed with 30 mM PBS buffer (pH 7.4) three times; then, 40 µL of RBCs were placed into a 1.5 mL tube and were lysed with ice cold 1160 µL of 3 mM PBS buffer (pH 7.4) for 10-15 minutes. The tube was centrifuged at 15000 x g at 4 °C for 10 minutes. The process was repeated several times. Then, 50 µL of the supernatant was taken and 50 µL 30 mM PBS buffer was added and microvortexed to mix. The aliquot of supernatant was diluted 200-fold with 5 mM aqueous ammonium acetate buffer and the hemolysate was desalted using the Microcon YM-10 centrifugal filters.

3.2.3.3 Patients' Blood Sample Preparation

Blood samples from the colorectal cancer patients undergoing chemotherapy treatment with oxaliplatin were collected at the Cross Cancer Institute (Edmonton, AB,

Canada). Written informed consents were obtained from the patients. The RBC and plasma of patients' blood samples were obtained using the freezing/thawing method, as described in Section 3.2.3.2.

3.3 Results and Discussion

3.3.1 NanoESI-MS Study of Hb-Drug Complexes Formed *in vitro*

The reaction mixtures, containing a constant concentration of 10 μM Hb with increasing concentration of 0, 10, 50, and 100 μM oxaliplatin incubated at 37 °C, were monitored by nanoESI-MS. Figure 3.1 shows the mass spectra of mixtures of oxaliplatin with Hb at different molar ratios after 24 hours incubation. The three distinctive peaks in Figure 3.1a are the charge state 19+, 18+, and 17+ ions of the Hb tetramer control. When equal moles of oxaliplatin and Hb (molar ratio 1:1) were incubated, one extra spectral peak was observed besides each peak of the Hb tetramer in Figure 3.1b. This extra spectral peak suggested that one new species (labelled peak 1) was detected. With an increased oxaliplatin:Hb molar ratio to 5:1, besides each of the Hb tetramer peaks, two extra peaks were observed in Figure 3.1c. This suggests that another new species (labelled peak 2) was detected in addition to new species peak 1. Furthermore, when the oxaliplatin:Hb molar ratio was increased to 10:1, three extra peaks besides each peak of the Hb tetramer were visible in Figure 3.1d. This suggests that another new species (labelled peak 3) was detected, in addition to new species peak 1 and peak 2. Table 3.1 lists the measured m/z value of charge state 19+, 18+, and 17+ of the Hb tetramer and new species detected in the spectra b), c), and d) of Figure 3.1.

To identify these new species, we transformed the raw mass spectra into the deconvoluted mass spectra so that we could obtain the molecular mass of these species. Figure 3.2 shows the deconvoluted mass spectrum of a) the Hb control and b) the reaction mixture of Hb with oxaliplatin at molar ratio 10:1 incubated for 24 hours. Figure 3.2b showed that the measured molecular mass of the intact Hb tetramer was 64457 Da, the molecular mass of the species peak 1 was 64764 Da, and the molecular mass of the species peak 2 was 65072 Da. The measured mass difference between the species peak 1 and the Hb tetramer was 307 Da. The molecular mass of the whole drug Pt(DACH)(oxalate) is 397.3 Da. As mentioned in Chapter 1, oxaliplatin may be transformed into the hydrated species: $Pt(DACH)(H_2O)_2$, which reacts with amino acids or proteins by the loss of two H_2O resulting in the form of Pt(DACH)- in the complex. The calculated molecular mass of Pt(DACH)- is 307.3 Da. Therefore, the measured mass difference between the species peak 1 and the Hb tetramer corresponds to the mass increment of Pt(DACH)-, which suggests that one drug molecule binds to the Hb to form a Hb-1drug complex in the form of Hb-Pt(DACH). Furthermore, the measured mass difference of the species peak 2 and the species peak 1 (identified as Hb-1drug complex) was 308 Da, which is very close to the calculated molecular mass of Pt(DACH)-. It suggests that two drug molecules bind to the Hb to form a Hb:2drug complex in the form of Hb-$[Pt(DACH)]_2$. Therefore, the three new species were identified as the Hb-oxaliplatin complexes with a binding stoichiometry of Hb-1drug complex, Hb-2drug complex, and Hb-3drug complex.

Comparing mass spectrum c) with d) in Figure 3.1, it was found that increasing the oxaliplatin:Hb molar ratio from 5:1 to 10:1 not only resulted in an increased number

of drug molecules bound to each Hb tetramer (from 2 to 3), but also led to an increase in the relative intensity of Hb-oxaliplatin complexes. The relative ratio of the Hb:1drug complex was increased from 52% to 95% and that of the Hb:2drug complex from 10% to 30%. We observed different amounts of different types of Hb:drug complexes using nanoESI-MS after incubation of oxaliplatin with intact Hb at different molar ratios. This may suggest that the Hb-oxaliplatin complexes detected were not artifacts in the gas phase generated during the electrospray process. Our results obtained by nanoESI-MS revealed that the intact Hb tetramer formed drug complexes with oxaliplatin after *in vitro* incubation.

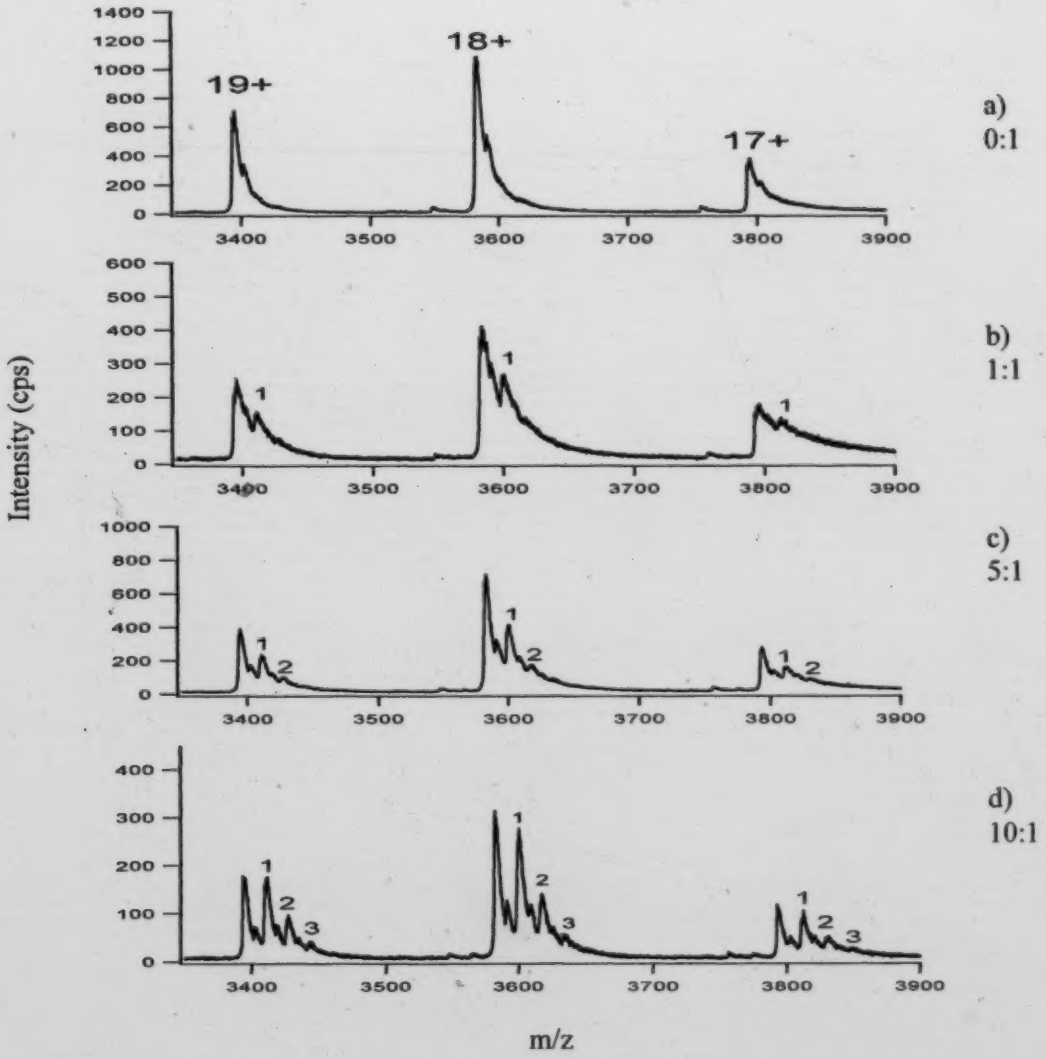

Figure 3.1 Typical nanoESI mass spectra of oxaliplatin-Hb complexes formed in reaction mixtures of oxaliplatin and Hb at oxaliplatin:Hb molar ratio of a) 0:1 , b) 1:1 , c) 5:1 , d) 10:1 . The reaction mixtures of oxaliplatin and Hb were incubated at 37 °C for 24 hours. The additional peaks labelled 1, 2, and 3 indicate three different Hb-drug complex species.

Table 3.1 Measured m/z value of Hb and the three new species in Figure 3.1

	Species	Charge state	Measured m/z	Calculated M/z	Mass Accuracy ppm
b)	Hb	19+	3394.6	3393.3	383
oxaliplatin:Hb		18+	3581.9	3581.7	56
1:1 molar ratio		17+	3795.8	3792.4	896
	Peak 1	19+	3414.8	3409.4	1584
	(Hb-1drug)	18+	3598.9	3598.8	28
		17+	3812.9	3810.4	656
c)	Hb	19+	3394.5	3393.3	354
oxaliplatin:Hb		18+	3583.2	3581.7	419
5:1 molar ratio		17+	3793.6	3792.4	316
	Peak 1	19+	3410.8	3409.4	411
	(Hb-1drug)	18+	3600.5	3598.8	472
		17+	3813.4	3810.4	787
	Peak 2	19+	3431.2	3425.6	1635
	(Hb-2drug)	18+	3617.5	3615.8	470
		17+	3828.8	3828.5	78
d)	Hb	19+	3393.3	3393.3	10
oxaliplatin:Hb		18+	3581.8	3581.7	28
10:1 molar ratio		17+	3792.4	3792.4	10
	Peak 1	19+	3410.4	3409.4	293
	(Hb-1drug)	18+	3599.8	3598.8	277
		17+	3811.9	3810.4	394
	Peak 2	19+	3427.5	3425.6	555
	(Hb-2drug)	18+	3618.2	3615.8	664
		17+	3832.5	3828.5	1045
	Peak 3	19+	3437.9	3441.7	1104
	(Hb-3drug)	18+	3634.2	3632.9	358
		17+	3851.9	3846.5	1404

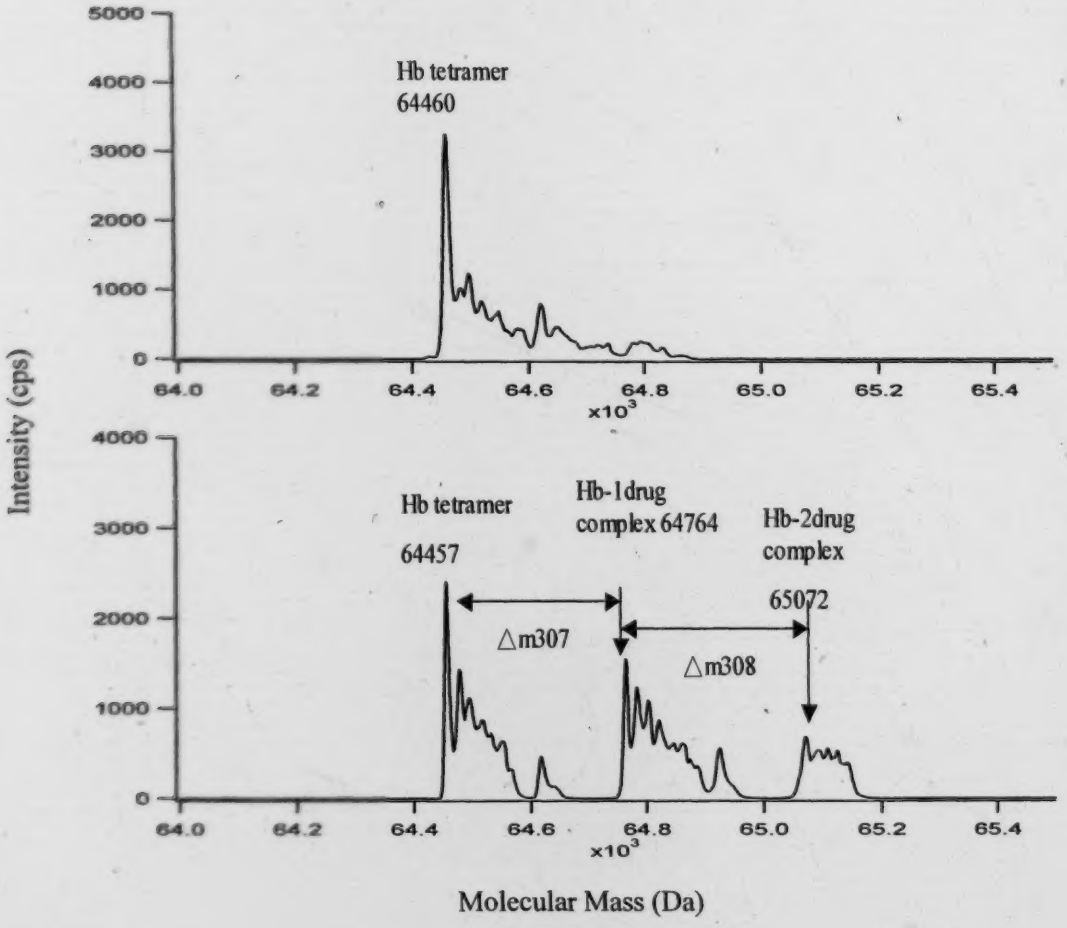

Figure 3.2 Deconvoluted mass spectra of the Hb tetramer control and the reaction mixture of oxaliplatin with Hb at molar ratio 10:1 incubated for 24 hours. The mass difference between Hb-1drug complex and Hb is 307 Da, which corresponds to the calculated molecular mass of hydrated drug loss of 2 H_20: Pt(DACH)- (the calculated molecular mass 307.3 Da). The mass difference between Hb-2drug complex and Hb-1drug complex is 308, which also corresponds to the calculated molecular mass of hydrated drug loss of 2 H_20: Pt(DACH)-.

To explore the effect of incubation time on the formation of Hb-oxaliplatin complexes, we incubated the Hb with oxaliplatin at different molar ratios at 37 °C for 5 days. Figure 3.3 shows the mass spectra of the mixture of Hb (10 μM) with different amount of oxaliplatin after 5 days of incubation at 37 °C. It was found that an even larger number of Hb-oxaliplatin complex species were detected after 5 days than after 24 hours. At oxaliplatin:Hb molar ratio of 1:1, two additional peaks besides each of the peaks of Hb tetramer were observed (Figure 3.3b), which indicated that the species peak 2 was detected in additional to the species peak 1. In Figure 3.3b, the Hb tetramer was still the predominant species. At oxaliplatin:Hb molar ratio of 5:1, another new species peak 3 was detected in additional to peak 1 and peak 2 (Figure 3.3c). In this spectrum, it was obvious that the ion intensity of the species peak 1 was higher than the Hb tetramer and became the predominant species. At oxaliplatin:Hb molar ratio of 10:1, six additional peaks besides each peak of the Hb control were observed (Figure 3.3d), which suggested that additional species peak 4, peak 5 and peak 6 were detected. Figure 3.3d clearly shows that the ion intensity of the Hb tetramer was the lowest and that the species peak 3 was the predominant species. Based on their measured mass difference, these new species were also identified as Hb-oxaliplatin complexs. Peaks 1, 2, 3, 4, 5, and 6 represent the species Hb-1drug complex, Hb-2drug complex, Hb-3drug complex, Hb-4drug complex, Hb-5drug complex, and Hb-6drug complex, respectively. This study suggests that prolonged incubation times increased formation of Hb-oxaliplatin complexes.

Up to six drug molecules were found to be bound to each Hb tetramer molecule after 10-fold molar excess of oxaliplatin was incubated with Hb for 5 days. However, this study did not provide information about the specific binding site in the Hb.

The established nanoESI-MS method can differentiate the intact Hb tetramer and Hb-oxaliplatin complexes; therefore, we can easily determine the binding stoichiometry of oxaliplatin bound to the intact Hb tetramer. The binding stoichiometry of oxaliplatin with intact Hb depends on several factors, such as the different molar ratio or different incubation time. When the results from 5 days incubation were compared with those from 24 hours incubation, the data show that the formation of Hb-oxaliplatin complexes can be more easily detected with the increased drug concentrations and incubation time.

There is some evidence to support the specificity of Hb-oxaliplatin complexes detected by nanoESI-MS. In our study, ultrafilter device (molecular weight cut-off 10K Da) was used to remove the unbound drug and only the fraction containing the Hb and Hb-drug complexes was subject to nanoESI-MS analysis. Because the unbound drug was gone, then the gas phase adduct ions should not occur and Hb-oxaliplatin complexes ions were by far more specific. The Hb-oxaliplatin complexes were detected using the 5 mM aqueous ammonium acetate (pH around 7), and our laboratory also detected that the oxaliplatin binds to both subunits α, β-chains using acidic solution (pH around 2). Thus the Hb-oxaliplatin complexes were detected using different solution condition. If the Hb-oxaliplatin complexes were not specific, there would have not been detected under different solution conditions. More amount of Hb-oxaliplatin complexes were detected after longer incubation time (5 days compared to 24 hours). These evidence suggests that the Hb-oxaliplatin complexes are specific, not the artifact ions in the gas phase.

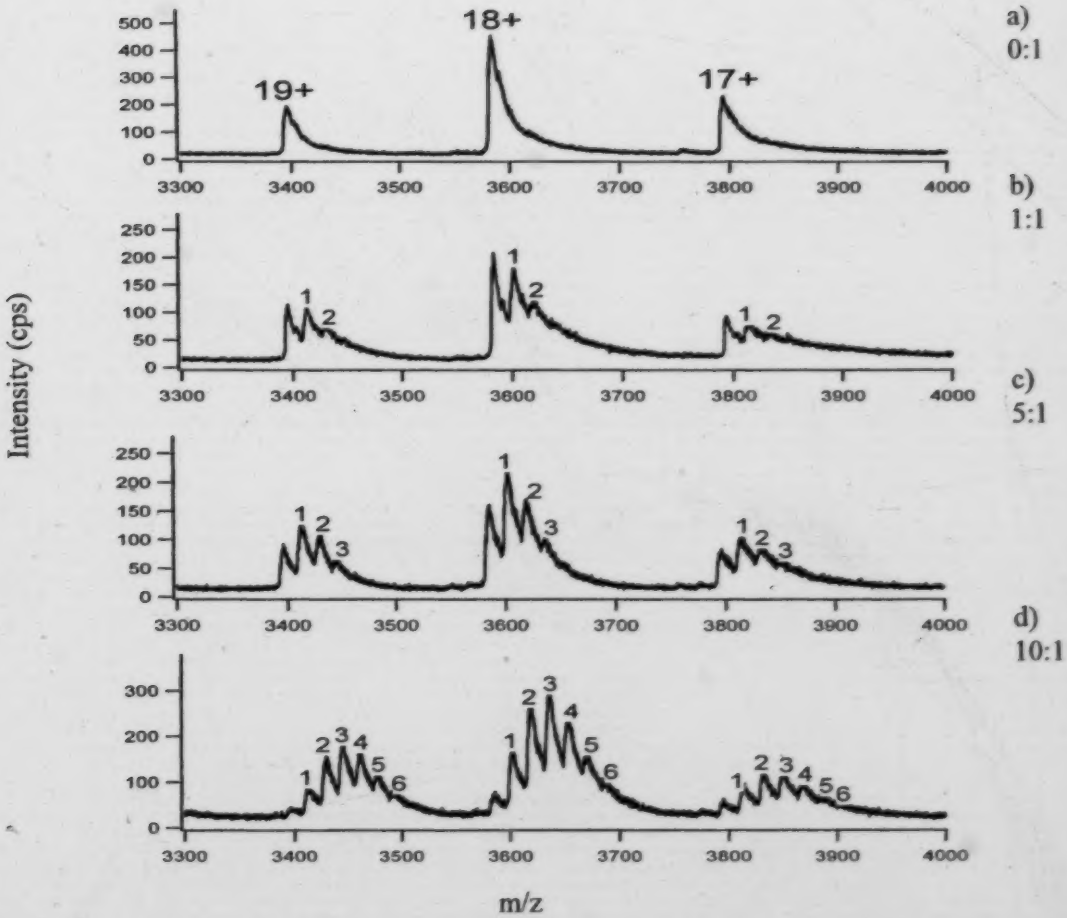

Figure 3.3 Typical nanoESI mass spectra of oxaliplatin-Hb complexes formed in reaction mixtures of oxaliplatin and Hb at oxaliplatin:Hb molar ratio of a) 0:1, b) 1:1, c) 5:1, and d) 10:1. The reaction mixtures were incubated at 37°C for 5 days. The peaks labelled 1, 2, 3, 4, 5, and 6 indicate the different species of Hb-1drug , Hb-2drug, Hb-3drug, Hb-4drug, Hb-5drug and Hb-6drug complex, respectively.

3.3.2 Characterization of Hb-Oxaliplatin Complexes by Tandem MS

3.3.2.1 Tandem MS Study of Hb Dimer-Oxaliplatin Complexes

To further identify and characterize the structure of Hb-oxaliplatin complexes, tandem mass spectrometry with collision-activated dissociation (CAD) was used to study the gas phase dissociation of Hb-oxaliplatin complexes. The QSTAR Pulsar i quadrupole/time-of-flight has a m/z limit of 3000 for Q1 and, as a result, the precursor ions with a mass to charge ratio of greater than 3000 cannot be selected for MS/MS experiments. Therefore, we studied the fragmentation of the oxaliplatin complexes of the Hb dimmer (αhβh), which were in the m/z range of 2000-3000. Figure 3.4 shows the nanoESI-MS spectrum of Hb dimmer-oxaliplatin complexes. The peak at m/z 2480 corresponds to a charge state 13+ ion of the Hb dimer and the peak at m/z 2504 corresponds to a charge state 13+ ion of the Hb dimmer-oxaliplatin complex. The peak at m/z 2686 corresponds to a charge state 12+ ion of the Hb dimer and the peak at m/z 2714 corresponds to a charge state 12+ ion of the Hb dimmer-oxaliplatin complex.

We chose these four peaks as precursor ions to obtain the product ions of Hb dimer and Hb dimmer-oxaliplatin complexes.

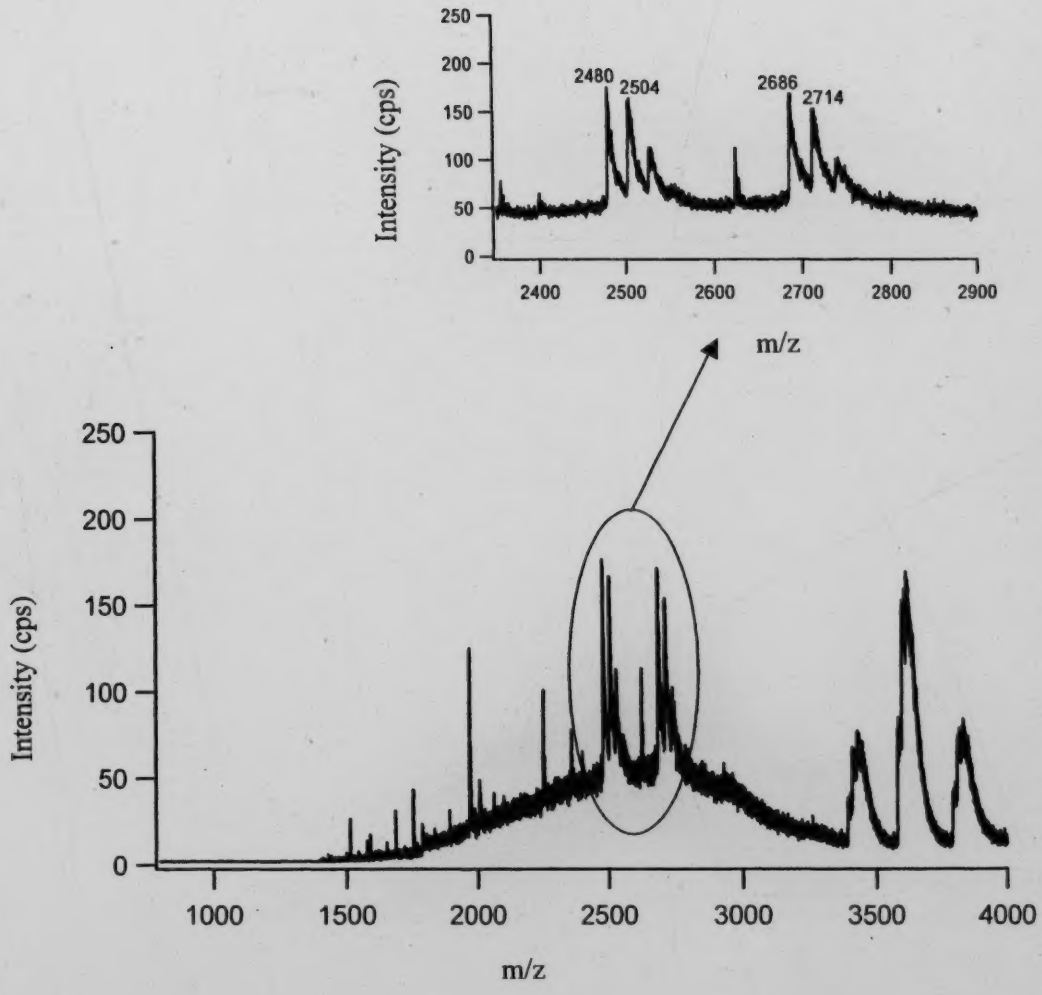

Figure 3.4 NanoESI mass spectrum of the Hb dimer and dimmer-oxaliplatin complexes formed in a reaction mixture of Hb with oxaliplatin molar ratio 1:1 incubated for 24 hours. The peaks at m/z 2480, 2504, 2686, and 2714 indicate the charge state 13+ and 12+ ions of the Hb dimer (αhβh) and the Hb dimer-drug complexes, respectively.

Figure 3.5 showed the product ion spectra of a) the precursor ion m/z 2686 of Hb dimmer (charge state 12+ ion of αhβh) and b) the precursor ion m/z 2714 of Hb dimmer-drug complex (charge state 12+ of αhβh-drug), which were obtained at a collision energy 80 eV and a collision gas 9. The MS/MS spectrum of the Hb dimer (Figure 3.5a) showed that the precursor ion was fragmented into a series of multiply charged ions of the α-chain and β-chain as well as the heme group, among which α8+ and β8+ ions were the most abundant peaks. The MS/MS spectrum of the Hb dimmer-drug complex (Figure 3.5b) showed that the precursor ion was fragmented into α-drug complex ion, β-drug complex ion as well as α-chain and β- chain ions. The ions indicated by arrow were the most abundant peaks, which are the charge state 8+ of α-drug complex and the charge state 8+ of β-drug complex.

We transformed the raw product ion spectra to deconvoluted mass spectra using Analyst QS software from Applied Biosystems. The deconvoluted product ion spectrum of the precursor ion 2714 m/z was shown in Figure 3.6. It clearly showed that the measured molecular mass of α-polypeptide chain and β-polypeptide chain was 15125.8 and 15867.2 Da, respectively. Furthermore, besides the peak of α-chain there was one distinctive peak at 15433.0 Da and besides β-chain there was one additional peak at 16147.6 Da. The mass difference between α-chain and α-drug complex was 307.2. The mass difference between β-chain and β-drug complex was 307.4 Da. The calculated molecular mass of the parent drug oxaliplatin is 397.3 Da and the calculated molecular mass of Pt(DACH)-, which is the hydrated species by the loss of 2 H_2O, is 307.3 Da. Therefore, the MS/MS study suggests that the main species of drug which was bound to

the Hb dimer was Pt(DACH)-. This result confirms that the oxaliplatin binds to the Hb and the hydrated species of the drug form the Hb-drug complexes with the Hb.

Our MS/MS spectra of charge 12+ and 13+ ions of the Hb dimer were consistent with the spectra by the previous study [21]. As we mentioned earlier, the α- and β-chains associate into dimer through noncovalent binding and heme also noncovalently binds to α- and β-chains. Under relatively high collision energy (collision energy 80 eV and collision gas value 9), the Hb dimer was fragmented to α- and β-chains and heme was also released from α- or β-chains. From the MS/MS spectra of the precursor ion m/z 2714, the charge state 12+ ion of the Hb dimer-drug complex, we particularly detected the ions of α-drug complex and β-drug complex. These findings confirmed that the selected precursor ion m/z 2714 was indeed the ion of the Hb dimer-drug complex. The formation of the Hb dimmer-drug complex was the specific binding between the Hb and oxaliplatin. Figure 3.6 shows that after dissociation of the Hb dimer-drug complexes in the gas phase, the dominant fragment species was α-chain and β-drug complex, suggesting that oxaliplatin was preferably bound to β-chain. It is notable that the heme group was fragmented from the α-chain and β-chain under this relatively high collision condition, whereas, the drug was still bound to the α-chain and β-chain. This may suggest that the binding between the drug and α-chain and β-chain is stronger than the binding between heme and α-chain and β-chain.

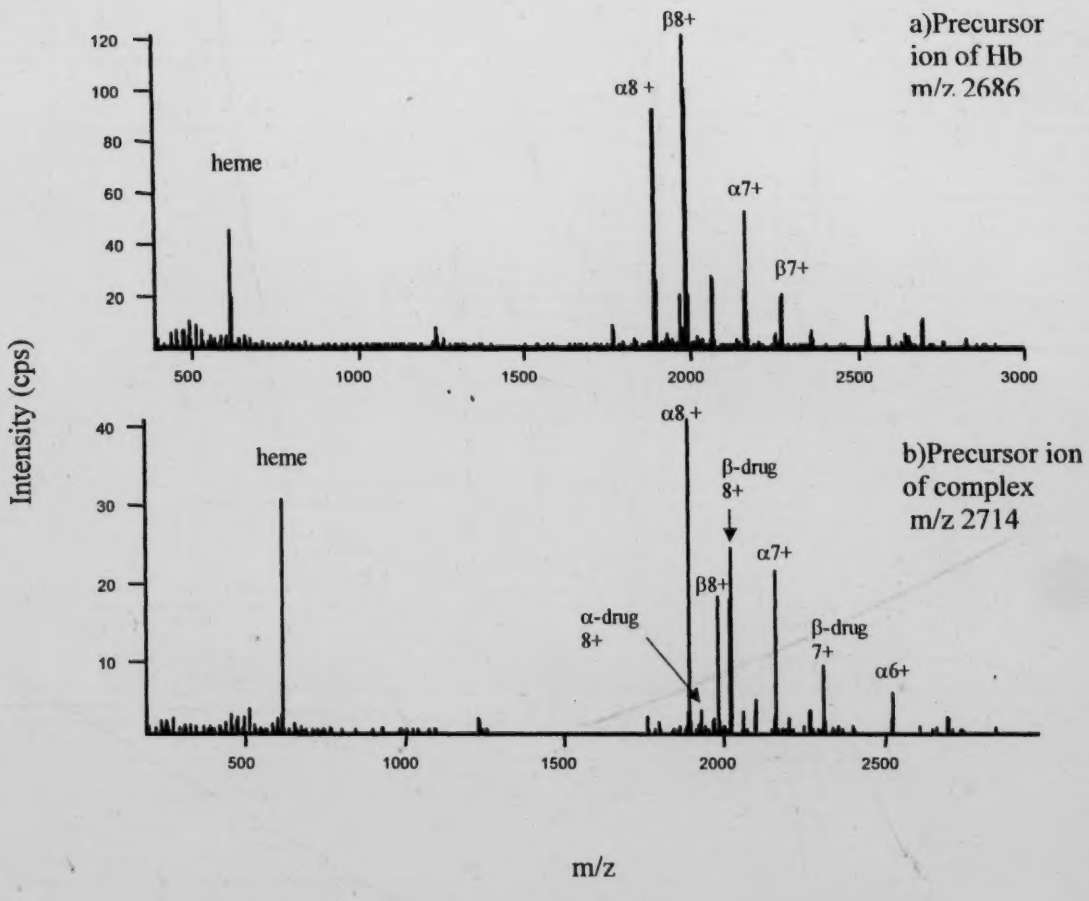

Figure 3.5 Product ion spectra of a) precursor ions of Hb dimmer (m/z 2686) and b) precursor ion of dimmer-drug complex (m/z 2714) obtained at a collision energy of 80 eV and collision gas setting of 9.

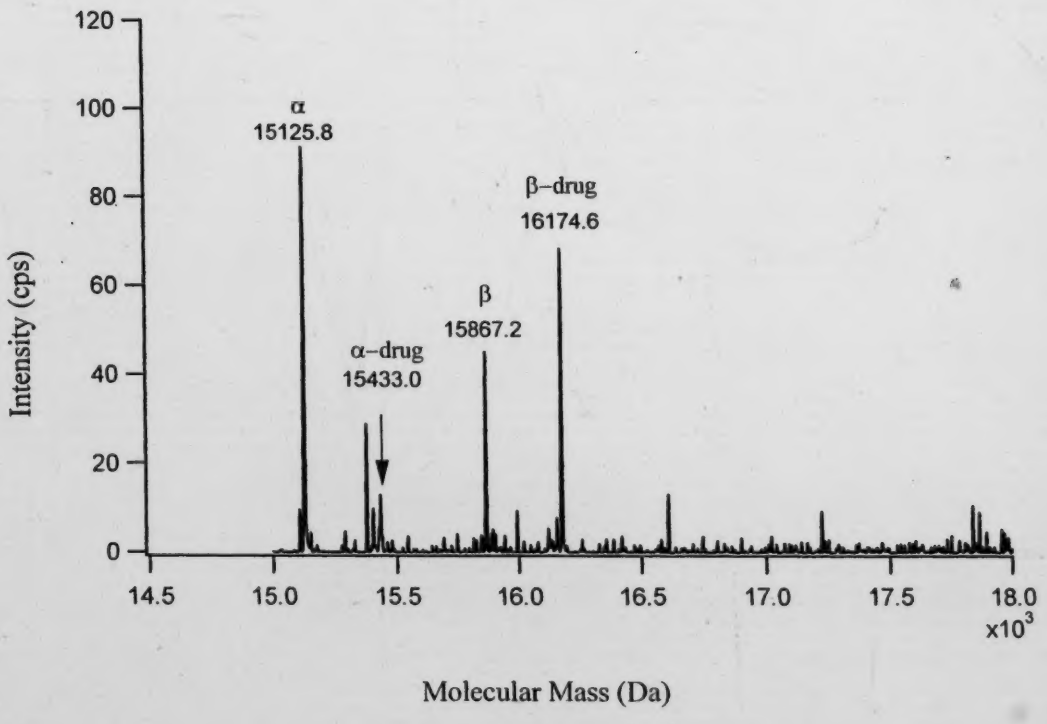

Figure 3.6 Partial deconvoluted product ion spectrum of precursor ion m/z 2714 (from molecular mass 14500 to 18000 Da). The molecular mass of α-chain and α-drug is 15125.8 and 15433.0 Da, respectively, and the mass difference is 307.2 Da. The molecular mass of β-chain, β-drug is 15867.2 and 16174.6 Da, respectively, and the mass difference is 307.4 Da.

3.3.2.2 Tandem MS Study of Hb Ttetramer-Oxaliplatin Complexes

In order to directly characterize the intact Hb tetramer-oxaliplatin complexes, a QSTAR XL Q-TOF mass spectrometer (Applied Biosystems/MDS Sciex), which has a higher mass range (up to m/z 4000) in Q1, was used to obtain the tandem mass spectrum. Figure 3.7 shows the product ion mass spectrum of the precursor ion m/z 3604, charge state 18+ ion of the intact Hb tetramer-oxaliplatin complexes, at CE 15 eV and 30 eV. At a CE value of 15 eV, charge state 18+ ions of the Hb tetramer-oxaliplatin complex were fragmented to mainly the Hb monomers in the mass range of m/z 1000-2500; however, no fragment ion of parent drug oxaliplatin was observed (Figure 3.7a). At a CE value of 30, a significant amount of fragment ions were observed at low mass range (m/z 200-500) in Figure 3.7b. The expanded mass spectrum of m/z 350-450 (Figure 3.7c) clearly shows the isotope pattern of the parent drug oxaliplatin. The observation of the parent drug oxaliplatin in the product ion mass spectrum confirmed that the parent drug oxaliplatin was bound to the intact Hb tetramer.

When we further examined the mass spectrum in the mass range of m/z 1650-1800 (Figure 3.8), it showed that α9+ and β9+ were the predominant fragment ions and more interestingly there were some additional peaks besides each of the main peaks α9+ and β9+. These additional peaks were identified as charge state 9+ ions of [α-Pt(DACH)], [α-Pt(DACH)(Oxalate)] and [β-Pt(DACH)], [β-Pt(DACH)(Oxalate)]. The detection of the fragment ions [α-Pt(DACH)] and [β-Pt(DACH)] confirmed again that hydrated drug species of oxaliplatin was also bound to the intact Hb tetramer.

The tandem MS studies of the Hb dimer-oxaliplatin complexes and the Hb tetramer-oxaliplatin complexes formed *in vitro* confirm that both the parent drug Pt(DACH)(oxalate) and the hydrated drug Pt(DACH)$(H_2O)_2$ formed complexes with the intact Hb tetramer. The parent drug oxaliplatin ions, which were fragmented from the Hb-drug complex, were detected in the MS/MS spectrum, while the hydrated drug ions were not detected and instead the hydrated drug bound to the Hb α-chain or β-chain were detected in the MS/MS spectrum. These results may suggest that the binding between the hydrated drug and Hb is stronger than the binding between parent drug and Hb.

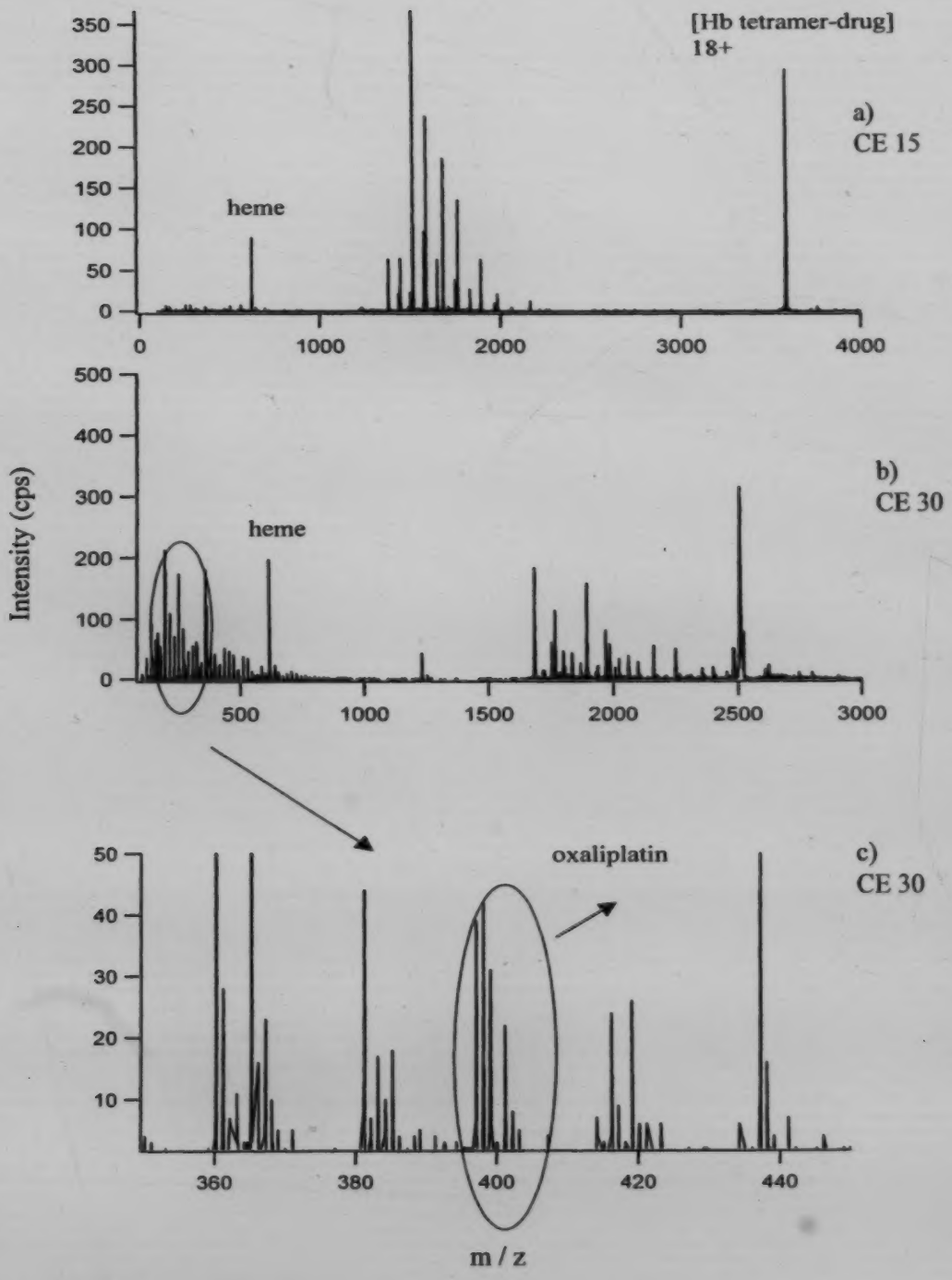

Figure 3.7 Product ion mass spectrum of precursor ion charge state 18+ of the Hb tetramer-oxaliplatin complexes a) at CE 15 eV; b) at CE 30 eV; c) expanded mass range to show the presence of parent drug oxaliplatin ions at CE 30 eV.

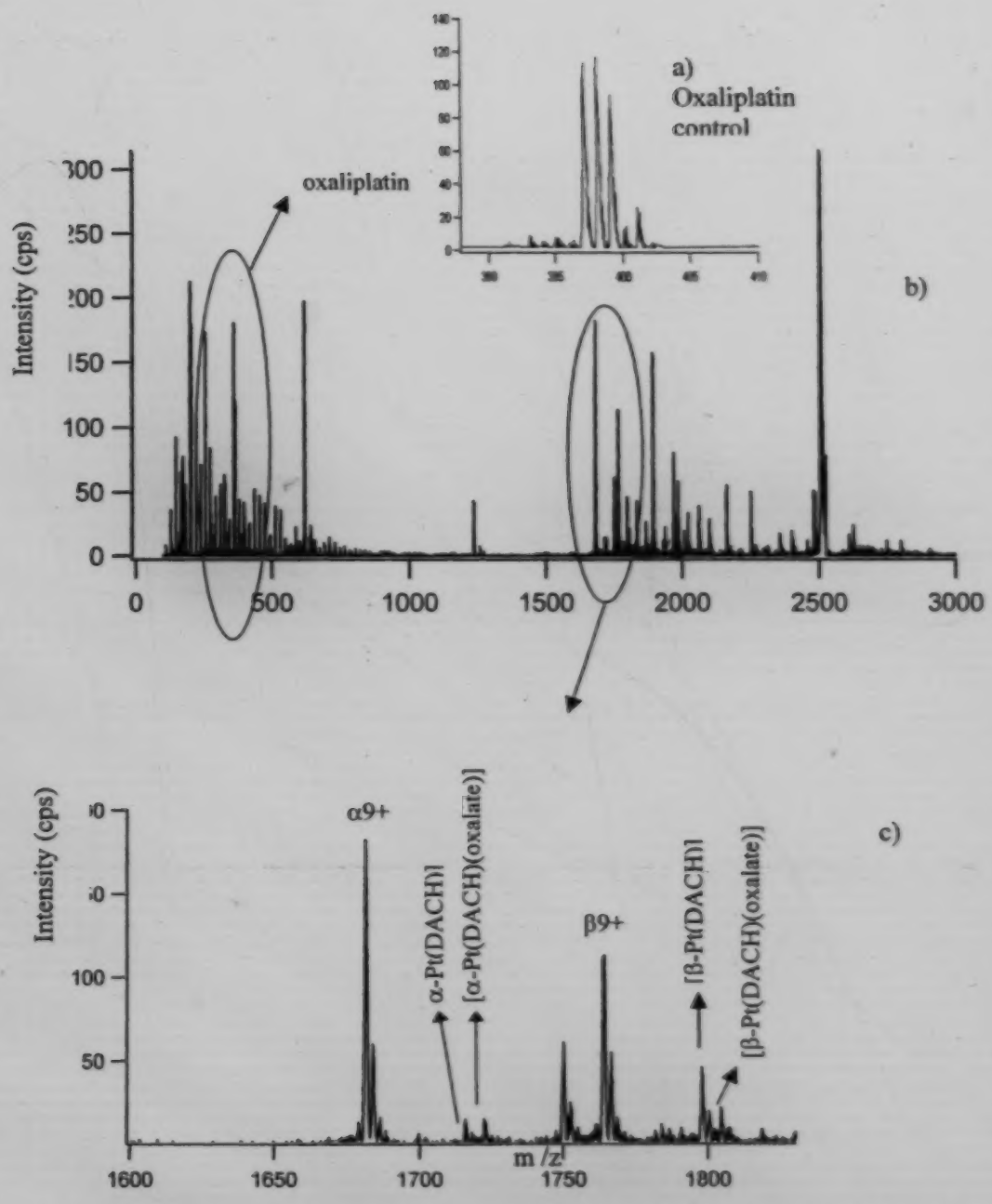

Figure 3.8 a) ESI mass spectrum of oxaliplatin control, b) product ion spectrum of charge 18+ Hb-drug complex, c) expanded product ion spectrum shows additional fragment ions, which are [α-Pt(DACH)], [α-Pt(DACH)(Oxalate)] and [β-Pt(DACH)], [β-Pt(DACH)(Oxalate)].

Table 3.2. Measured mass-to-charge ratios and mass accuracy of the fragment ions of the drug complexes formed in the incubated solution of Hb and oxaliplatin (Figure 3.8).

Species	m/z (Theoretical)	m/z (Experimental)	Mass Accuracy (ppm)
Precursor: Hb tetramer-oxaliplatin complex	3603.78	3603.75	8
α^{9+}	1681.67	1681.66	-5
β^{9+}	1764.00	1764.08	-46
heme α^{9+}	1750.11	1749.95	-93
heme β^{9+}	1832.44	1832.44	-2
α^{8+}	1891.75	1891.77	10
heme α^{8+}	1968.75	1968.79	21
heme β^{8+}	2061.37	2061.22	-72
Complex fragment ions			
α^{9+}	1715.78	1715.81	18
α^{*9+}	1725.76	1725.69	-39
β^{9+}	1798.11	1798.16	30
β^{*9+}	1808.11	1808.08	-18

α = [α-Pt(DACH)], α^* = [α-Pt(DACH)(Oxalate)]

β = [β-Pt(DACH)], β^* = [β-Pt(DACH)(Oxalate)].

3.3.3 Detection of Hb-Oxaliplatin Complexes in Patients' Blood Samples

3.3.3.1 Comparison of Two Red Blood Cell Lysis Methods

In order to ensure proper preparation of RBC for detection of the Hb-drug complexes formed *in vivo* in the patients' blood, we first examined two common lysis methods: freezing/thawing method and the hypotonic solution method [26]. We first prepared the hemolysate of RBCs from a normal adult human control using the two lysis methods and detected the hemoglobin tetramer using the established nanoESI-MS method. Figure 3.9 compared the two mass spectra of the RBCs hemolysate obtained from one healthy volunteer using: a) hypotonic solution method and b) freezing/thawing method. The three distinctive peaks observed in the spectra a) and b) correspond to the three different charge state of the intact Hb tetramer, which are consistent with the spectrum of the HbA0 standard (Figure 2.1b in Chapter 2). Therefore, we can detect the intact Hb tetramer from the hemolysate using these two methods. The hypotonic solution contains a phosphate buffer, which will suppress the ion signal intensity of the Hb tetramer and must be removed before ESI-MS. The removal of the phosphate buffer before ESI-MS analysis makes sample preparation tedious. Therefore, we decided to use the freezing/thawing method to prepare the RBCs hemolysate from the patients' blood samples.

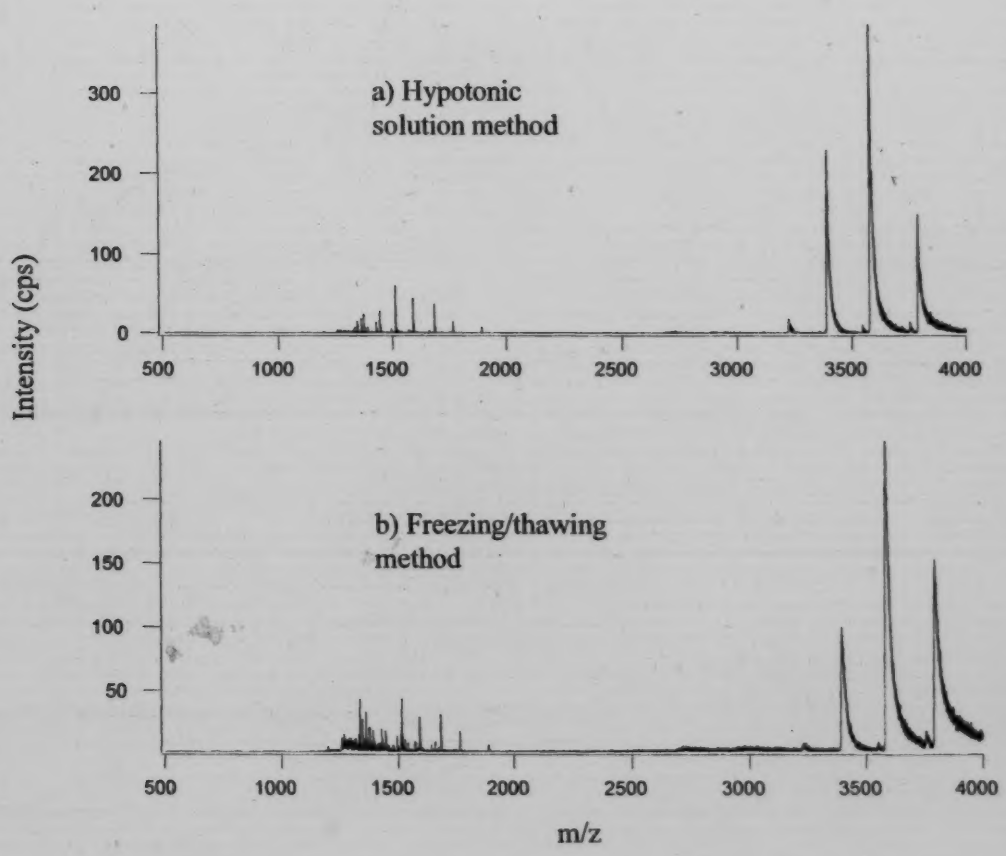

Figure 3.9 NanoESI mass spectra of the hemolysate of RBCs from one healthy volunteer using two lysis methods: a) hypotonic solution method and b) freezing/thawing method.

3.3.3.2 Detection of Hb-Oxaliplatin Complexes in Patients' Blood Samples

We applied the established nanoESI-MS method to detect the Hb-drug complexes in the RBCs hemolysate prepared using the freezing/thawing method. Figure 3.10 shows the mass spectra of the hemolysate from one patient's blood sample collected 1 hour and 48 hours after infusion. Spectrum a) is the mass spectrum of the hemolysate from a healthy volunteer, where the three distinctive peaks indicate the Hb tetramer itself. The spectra b) and c) show nanoESI mass spectra of RBCs hemolysate obtained from blood samples collected 1 hour and 48 hours after infusion, respectively. The spectra b) and c) clearly showed that there was an additional peak besides each of the three distinctive peaks of the intact Hb tetramer, which was labelled as arrows. This additional peak corresponds to the formation of the Hb tetramer-oxaliplatin complex, with a binding stoichiometry 1:1.

We carried out the tandem MS study of the Hb tetramer-drug complexes from the patients' RBC hemolysate to further characterize the structure of the drug complexes. The charge state 18+ ion (at m/z 3604) of the intact Hb tetramer-oxaliplatin complex was chosen as the precursor ion. Figure 3.11 showed that fragmented ions of parent drug oxaliplatin were observed in the product ion mass spectrum, and fragment ions of [α-Pt(DACH)], [α-Pt(DACH)(Oxalate)] and [β-Pt(DACH)], [β-Pt(DACH)(Oxalate)] were also observed. These results suggest that both the parent drug oxaliplatin and its hydrated species form the complexes with the intact Hb tetramer in patients' blood samples. The results were very consistent with the tandem MS study of the Hb tetramer-drug complexes formed *in vitro* incubation (Figure 3.8)

Compared the spectrum c) with b) in Figure 3.10, it was found that the similar amount of Hb-drug complexes were detected in patients' RBC samples collected at 1 hour and 48 hour after infusion. These suggest that these complexes formed in these patients' RBC were nearly stable over 48 hours relative to 1 hour.

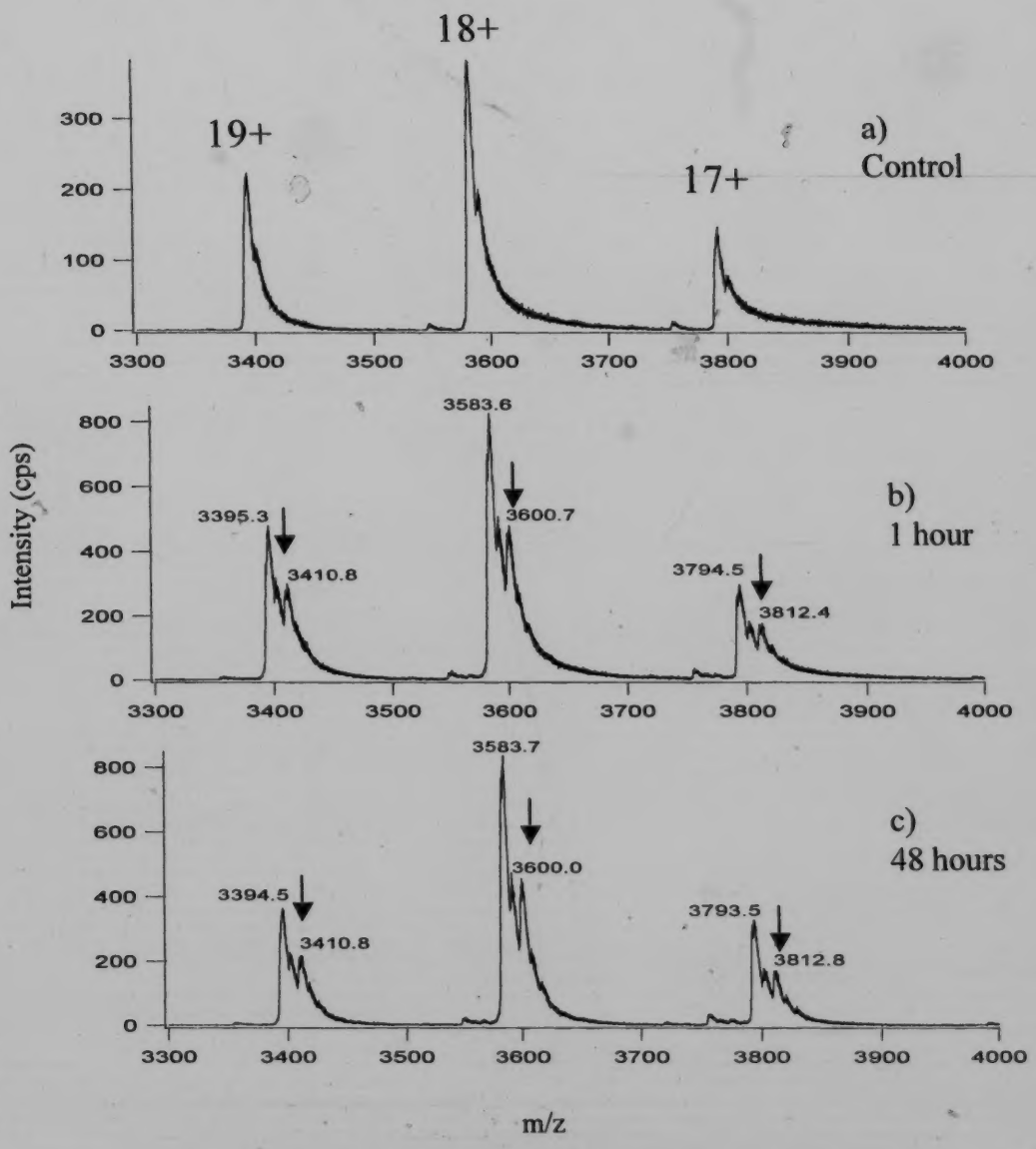

Figure 3.10 NanoESI mass spectra of Hb-oxaliplatin complexes in RBCs hemolysate from a cancer patient's blood sample: a) normal control; b) collected 1 hour after infusion; c) collected 48 hours after infusion.

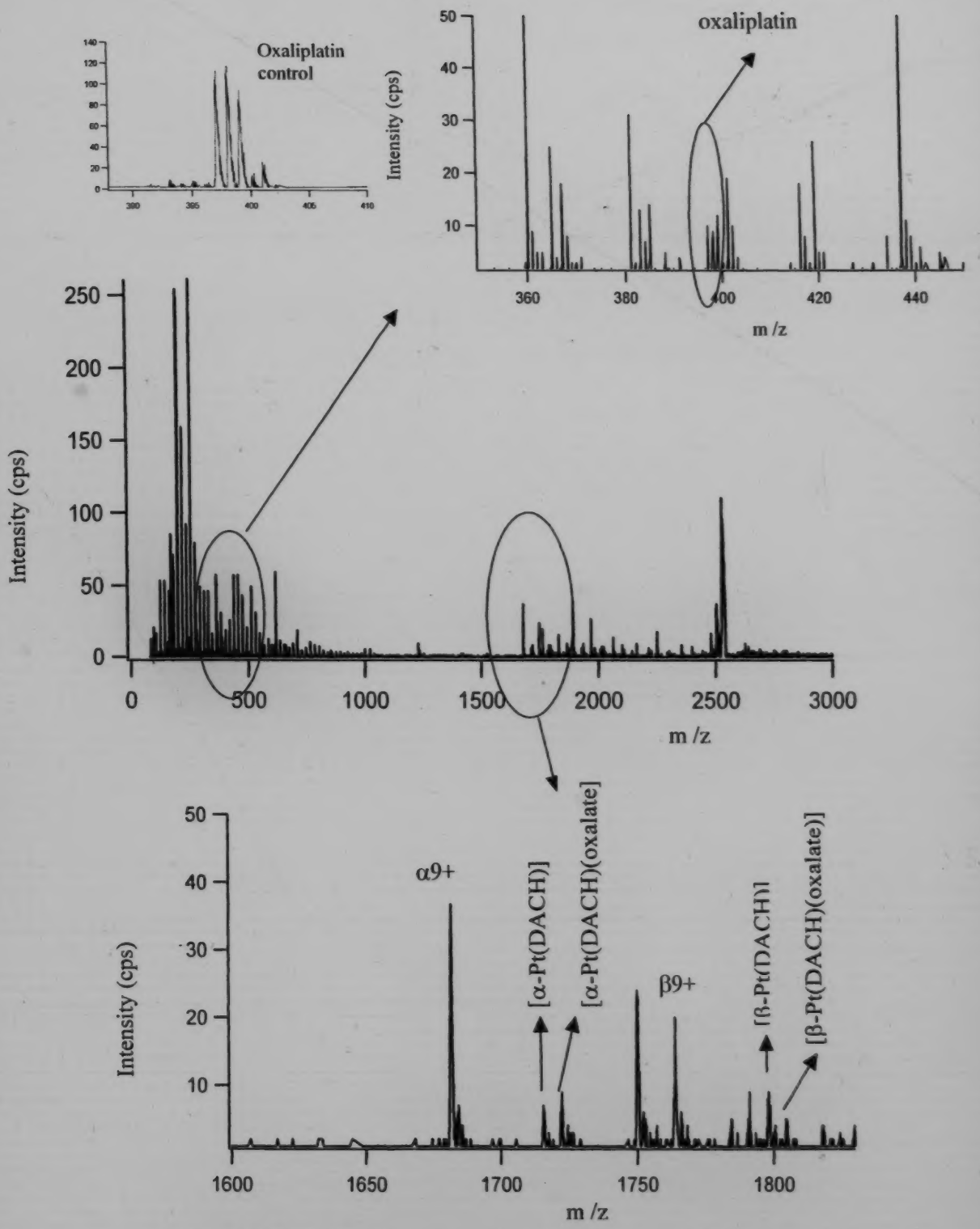

Figure 3.11 Product ion mass spectrum of the precursor ion charge state 18+ of the Hb tetramer-oxaliplatin complexes in a patient's blood sample.

Table 3.3 Measured mass-to-charge ratios and mass accuracy of the fragment ions of the intact Hb-oxaliplatin complexes formed in RBC (Figure 3.11).

Species	m/z (Theoretical)	m/z (Experimental)	Mass Accuracy (ppm)
Precursor: Hb tetramer-oxaliplatin complex	3603.77	3603.81	9
α^{9+}	1681.66	1681.63	-20
β^{9+}	1764.00	1763.93	-36
α^{8+}	1891.75	1891.71	-19
β^{8+}	1984.37	1984.31	-32
Complex fragments			
α^{9+}	1715.77	1715.64	-79
α^{*9+}	1725.75	1725.58	-97
β^{9+}	1798.11	1798.07	-21
β^{*9+}	1808.11	1808.06	-23

α = [α-Pt(DACH)], α^* = [α-Pt(DACH)(Oxalate)]

β = [β-Pt(DACH)], β^* = [β-Pt(DACH)(Oxalate)].

3.3.4 Detection of Serum Albumin-Oxaliplatin Complexes in Patients' Plasma Samples

After we established a methodology to detect the oxaliplatin-Hb complexes in RBC of cancer patients' blood samples, this work was extended to study the interaction of oxaliplatin with the main proteins in the plasma of cancer patients' blood samples using nanoESI-MS. Human serum albumin (HSA) (molecular mass of about 66437 Da), constituting about 4.5% of plasma, is the most abundant protein component in blood plasma [24]. HSA can bind to a variety of drug molecules including Pt-containing drugs and this binding could determine the drug's bioavailability and toxicity [25].

Figure 3.12 depicts the nanoESI mass spectra of HSA-oxaliplatin complexes in the plasma of the same patient's blood samples collected 1 hour after infusion and 48 hours after infusion. The three distinctive peaks predominant in the mass spectrum corresponded to the of HSA ions, which were the ions of the charge state 18+, 17+, and 16+. Besides each of the HSA peaks, there was one additional peak, which corresponded to the formation of an HSA-drug complex. By comparing the mass spectrum of the blood sample collected 1 hour after infusion with mass spectrum of the sample collected after 48 hours, it was found that the ion signal intensity of the HSA-drug complex significantly decreased and the relative intensity of drug complex to HSA decreased from approximately 60% to 35%. However, it is not easy to characterize the structure of HSA-oxaliplatin complexes from the mass difference due to the poor resolution of the mass spectra acquired in this study. Thus, tandem MS instrument that can select precursor ions above m/z 3000 is needed to further characterize the forms of the HSA-oxaliplatin complexes in the patients' plasma.

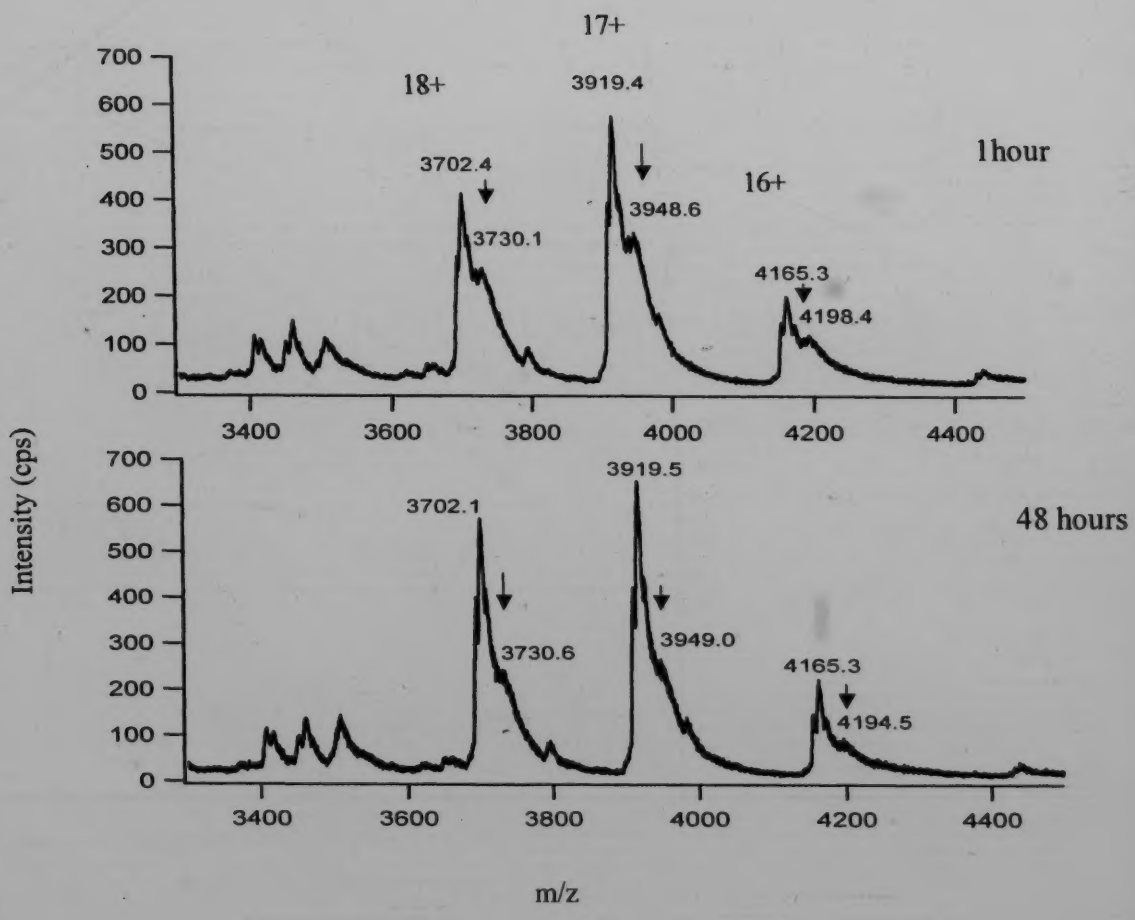

Figure 3.12 NanoESI mass spectra of serum albumin-oxaliplatin complexes in plasma from the same cancer patient's blood sample collected 1 hour after infusion and 48 hours after infusion. Each arrow represents the each series of peaks of HSA-1drug complex.

References

1. Graham J, Muhsin M, Kirkaptrick P. *Nat. Rev. Drug Discov.* 2004; 3: 11.
2. Francesco AMD, Ruggiero A, Riccardi R. *CMLS Cell. Mol. Life Sci.* 2002; 5: 1914.
3. Levi F, Metzger G, Massari C, Milano G. *Drug Dispos.* 2000; 38:1.
4. Raymond E, Faivre S, Chaney S, Woynarowski J, Cvitkovic E. *Mol. Cancer Ther.* 2002; 1: 227.
5. ReedijK J. *Chem. Rev.* 1999; 99: 2499.
6. Espinosa E, Feliu J, Zamora P, Baron MJ, Sanchez JJ, Ordonez A, Espinosa J. *Lung Cancer* 1995; 12: 67.
7. Appleton TG. *Coord. Chem. Rev.* 1997; 166: 313.
8. Pendyala L, Creaven PJ. *Cancer Res.* 1993; 53: 5970.
9. Allain P, Heudi O, Cailleux A, Bouil AL, Larra F, Boisdron-Celle M, Gamelin E. *Drug Metab. Dispos.* 2000; 28: 1379.
10. Gamelin E, Bouil AL, Boisdron-Celle M, Turcant A, Delva R, Cailleux A, Krikorian A, Brienza S, Cvitkovic E, Robert J, Larra F, Allain P. *Clin. Cancer Res.* 1997; 3: 891.
11. Timerbaev AR, Aleksenko SS, Polec-Pawlak K, Ruzik R, Semenova O. *Electrophoresis* 2004; 25: 1988.
12. Hagrman D, Goodisman J, Souid AK. *J. Pharmacol. Exp. Ther.* 2004; 308: 658.
13. Ivanov AI, Christodoulou J, Parkinson JA, Barnham KJ, Tucker A, Woodrow J, Sadler PJ. *J. Biol. Chem.* 1998; 273: 1472.
14. Gibson D, Costello CE. *Eur. Mass Spectrom.* 1999; 5: 501.

15. Peleg-Shulman T, Najajreh Y, Gibson D. *J. Inorg. Biochem.* 2002; 91: 306.

16. Allardyce CS, Dyson PJ, Coffey J, Johnson N. *Rapid Commun. Mass Spectrom.* 2002; 16: 933.

17. Heck AJR, Van den Heuvel RHH. *Mass Spectrom. Rev.* 2004; 23: 368.

18. Luo FR, Wyrick SD, Chaney SG. *J. Biochem. Mol. Toxicol.* 1999; 13:159.

19. Luo FR, Yen TY, Wyrick SD, Chaney SG. *J. Chromatogr. B* 1999; 724: 345.

20. Heudi O, Mercier-Jobard S, Cailleux A, Allain P. *Biopharm. Drug Dispos.* 1999; 20: 107.

21. Versluis C, Heck AJR. *Int. J. Mass Spectrom.* 2001; 210/211: 637.

22. Smith RD, Light-Wahl KJ. *Biol. Mass Spectrom.* 1993; 22: 493.

23. http://ca.expasy.org/cgi-bin/niceprot.pl?P68871 retrieved on March 20, 2005.

24. Meloun B, Moravek L, Kostka V. *FEBS Lett.* 1975; 58: 134.

25. Esposito BP, Najjar R. *Coord. Chem. Rev.* 2002; 232: 137.

26. Albert SN, Jain SC, Shibuya J, Albert CA. In *The Hematocrit in Clinical Practice* Thomas CC(ed). 1965.

Chapter 4 Summary and Future Work

This research dealt with some challenges in the mass spectrometry detection of intact hemoglobin, a noncovalent protein complex, and its glucose and drug complexes. A nanoelectrospray ionization quadrupole/time-of-flight mass spectrometry technique was successfully developed to simultaneously detect the intact hemoglobin tetramer and the glycated hemoglobin. The technique was further applied to study the interaction between the anticancer drug oxaliplatin and intact Hb to demonstrate its potential application in clinical study and drug development.

Chapter 2 described the procedure for the optimization of the experimental conditions, including the sample solution composition and instrumental conditions required to detect the noncovalent quaternary structure of the Hb tetramer. Critical instrumental parameters such as the collision energy, declustering potential, focusing potential, and collision gas setting were optimized to get a high resolution mass spectrum of the intact Hb tetramer complexes. This study reported that the simultaneous detection of the intact Hb tetramer and the glycated Hb was accomplished using the established nanoESI-MS method and the results demonstrated that the main glycated Hb species was one glucose molecule bound to each Hb tetramer molecule $(\alpha h \beta h)_2$-glucose.

Chapter 3 demonstrated the application of this nanoESI-MS method to study the interaction of the anticancer drug oxaliplatin with the intact Hb tetramer. NanoESI-MS results confirmed that oxaliplatin was bound to the intact Hb tetramer after *in vitro* incubation of oxaliplatin with Hb. The detection of the Hb-oxaliplatin complex was dependent on the different molar ratios of oxaliplatin:Hb and different incubation times. The binding stoichiometry was determined and at least six drug molecules were found to

be bound to the intact Hb tetramer. The tandem MS studies suggested that both the parent drug and hydrated species of oxaliplatin form the Hb-drug complexes after *in vitro* incubation. The intact Hb tetramer-oxaliplatin complexes were also detected in cancer patients' RBCs. The tandem MS studies of the Hb tetramer-oxaliplatin complexes formed in patients' RBCs were consistent with that formed *in vitro* incubation and both hydrated drug and parent drug were bound to the intact Hb tetramer. It was also found that the amount of Hb-oxaliplatin complexes was nearly constant over 48 hours relative to 1 hour in the patients' RBCs after infusion of oxaliplatin. Furthermore, the serum albumin-oxaliplatin complexes were also detected using this method in the cancer patient's plasma samples. The nanoESI-MS studies not only confirmed that the Hb in RBCs was bound to the oxaliplatin, but also characterized the molecular species of oxaliplatin involved in the binding to Hb. Our results demonstrate that nanoESI-MS is a useful analytical method for the detection and characterization of intact Hb tetramer-drug complexes. The work reported here was the first to detect and characterize the intact Hb tetramer-oxaliplatin complex using ESI-MS.

Human hemoglobin and serum albumin are the predominant proteins in the blood with which a platinum drug can interact. We already showed that both the parent drug and its hydrated species of oxaliplatin can form complexes with the intact Hb tetramer; however, it is not clear whether the parent drug oxaliplatin or hydrated drug form complexes with other proteins. The structure of the serum albumin-oxaliplatin complexes detected in patients' plasma needs to be further characterized. The binding behaviour of other Pt-containing drugs with the intact Hb tetramer and serum albumin is also unclear,

therefore, further study is needed to investigate the interaction of other platinum drugs with the Hb tetramer and serum albumin.

The established nanoESI-MS technique is not limited to study the protein complexes of glucose and drugs; it can also be used to study protein complexes of environmental toxicants. Protein complexes of environmental toxicants can be used as biomarkers of exposure assessment and have applications in molecular epidemiological studies. Many environmental toxicants can bind to Hb to form stable Hb complexes. Because Hb complexes are readily accessible, more abundant, have a known rate of turnover (around 120 days) and they are not subject to enzymatic repair, they have been of great interest as potential biomarkers of exposure assessment. To develop Hb complexes as biomarkers, it is important to study the complex formation of Hb with environmental toxicants. The established nanoESI-MS method will be useful to detect and characterize the Hb complexes of environmental toxicants. Therefore, this nanoESI-MS method will be potentially useful to develop the Hb complexes of environmental toxicants as biomarkers for exposure assessment. However, it is noteworthy that people usually are exposed to the small amount of environmental toxicants and we have to consider the analytical challenges when using this method.